

**Technical University of Crete  
Department of Electronic Engineers & Engineers of  
Computers**



**Diploma thesis**

**“Imaging System for the pupillary photomotor reflex  
meter analysis”**

Kavvadias Vasileios

Committee: Associate Professor Costas Balas (Supervisor)  
Professor Michalis Zervakis  
Assistant Professor. Mattias Bucher

Chania 2009

PROJECT P.R.I.M.A.  
**PROJECT P.R.I.M.A.**

**PUPILLARY**

**REFLEX**

**IMAGING**

**METER**

**ANALYSIS**

## **Ευχαριστίες**

Για την εκπόνηση αυτής της εργασίας θα ήθελα να ευχαριστήσω θερμά τον επιβλέποντα καθηγητή μου κ. Κωνσταντίνο Μπάλα για την εμπιστοσύνη που μου έδειξε από την αρχή και την πολύτιμη καθοδήγηση του κατά την εξέλιξη της εργασίας. Επίσης θέλω να ευχαριστήσω τους ανθρώπους του εργαστηρίου της Οπτοηλεκτρονικής και ιδιαίτερα τους υποψήφιους διδάκτορες Παπουτσόγλου Γεώργιο και Τσάπρα Αθανάσιο για την σημαντική και αυθόρμητη βοήθεια που μου έδωσαν όποτε χρειάστηκα, αλλά και για την ακεραιότητα του χαρακτήρα τους. Ευχαριστώ πολύ τους επιβλέποντες καθηγητές, κ. Μιχάλη Ζερβάκη και Ματία Μπούχερ που δέχθηκαν να συμμετάσχουν στην ακαδημαϊκή επιτροπή της διπλωματικής μου εργασίας.

Θέλω ακόμα να ευχαριστήσω πραγματικά μέσα από την καρδιά μου όλους τους ανθρώπους που με στηρίζουν ψυχικά όλα αυτά τα χρόνια. Την οικογένεια μου, που με τη συνεχή αγάπη και ενθάρρυνσή της με ενδυναμώνει καθημερινά να προχωράω μπροστά, καθώς και όλους τους φίλους μου, γιατί είναι μοναδικοί.

## Διπλωματική εργασία

### «Ανάπτυξη απεικονιστικού συστήματος για τη μελέτη του φωτοκινητικού αντανακλαστικού της οπτικής θηλής»

#### Περίληψη

Αντικείμενο της εργασίας αυτής είναι η ανάπτυξη ενός απεικονιστικού συστήματος για την μέτρηση των δυναμικών αντανακλαστικών της οπτικής θηλής (οφθαλμικής κόρης). Το σύστημα πρόκειται να χρησιμοποιηθεί για την μελέτη του φωτοκινητικού αντανακλαστικού καθώς και των συσχετιζόμενων με αυτό παθήσεων του εγκεφάλου και του αυτόνομου νευρικού συστήματος. Στόχος είναι η ανάπτυξη μη επεμβατικών μεθόδων διάγνωσης των παθήσεων αυτών και αντικειμενικής αξιολόγησης της αποτελεσματικότητας θεραπευτικών σχημάτων. Το πρωτότυπο απεικονιστικό σύστημα το οποίο αναπτύχθηκε στα πλαίσια της εργασίας αυτής επιτρέπει την μέτρηση των ακούσιων δυναμικών μεταβολών της οπτικής θηλής σε συνθήκες εξωτερικού οπτικού ερεθίσματος. Το σύστημα βασίζεται σε απεικονιστικό αισθητήρα με ευαισθησία στο ορατό και στο υπέρυθρο μέρος του φάσματος. Η θηλή απεικονίζεται αρχικά στο υπέρυθρο μέρος του φάσματος με την χρήση υπέρυθρου LED. Σε αυτή την φασματική περιοχή το αντανακλαστικό δεν λειτουργεί, καθιστώντας έτσι δυνατή την καταγραφή της μέγιστης διαμέτρου της κόρης. Στην συνέχεια ενεργοποιείται το οπτικό ερέθισμα (LED λευκού φωτός) με ταυτόχρονη και αυτοματοποιημένη ενεργοποίηση της καταγραφής εικόνων σε χρονική ακολουθία η οποία διαρκεί και μετά την άρση του οπτικού ερεθίσματος. Ο έλεγχος και ο συγχρονισμός των υπομονάδων του συστήματος γίνεται μέσω μικροελεγκτή και ειδικά αναπτυγμένου λογισμικού. Πέραν αυτού, το λογισμικό του συστήματος περιλαμβάνει την υλοποίηση κατάλληλου αλγορίθμου για την αυτόματη οριοθέτηση της κόρης στο σύνολο των καταγεγραμμένων εικόνων. Από τα δεδομένα αυτά υπολογίζεται η διάμετρος του κύκλου ο οποίος οριοθετεί βέλτιστα την κόρη και τελικά υπολογίζεται η καμπύλη διάμετρος-χρόνος σε συνθήκες εισαγωγής και άρσης του οπτικού ερεθίσματος. Τέλος, η καμπύλη αυτή προσομοιώνεται με κατάλληλη συνάρτηση και υπολογίζονται ποσοτικές παράμετροι οι οποίες εκφράζουν τα ακούσια κινητικά χαρακτηριστικά της κόρης του ματιού. Η συσκευή αξιολογήθηκε τεχνικά αλλά και σε προ-κλινικό επίπεδο σε μάτια εθελοντών. Η αξιολόγηση έδειξε ότι η συσκευή πληροί πλήρως τις σχεδιαστικές προδιαγραφές και ότι οι μετρήσεις χαρακτηρίζονται από μεγάλη επαναληψιμότητα και αξιοπιστία. Η αναπτυχθείσα συσκευή πρόκειται να χρησιμοποιηθεί για την μελέτη της έκφρασης διαφόρων παθήσεων όπως Alzheimer, εγκεφαλικοί όγκοι, τραύματα κλπ, στο μετρούμενο πλέον φωτοκινητικό αντανακλαστικό, με στόχο την ανάπτυξη και εισαγωγή νέων-μη επεμβατικών διαγνωστικών κριτηρίων και μεθόδων για τις παθήσεις αυτές.

## **Diploma thesis**

### **“Imaging System for the pupillary photomotor reflex meter analysis”**

#### Abstract

The objective of this study is the creation of a digital imaging system, able of measuring the pupillary reflexes with accuracy. The device is designed for the practical examination of the pupillary light reflexes and the swinging flashlight test. It is indented to serve as a novel mean for non-invasive diagnosis and therapeutical methods evaluation. The prototype model was developed after extensive bibliographic research on pupillography. Materials include, briefly, digital cameras, infrared and visible illumination emitters, a microcontroller and optical filters. A custom image processing algorithm was developed to calculate pupil's diameter and a new approach was made concerning curve fitting and derivation of the resulting pupillogram. Results provide a wide range of information on the pupil's sensitivity, latency and mobility according to recent lateralization parameters. Digital pupillography presents a relatively simple and real time window for the autonomous nervous system functionality with an uprising research interest in various clinical studies.

## Table of Contents

<b>1. Introduction.....</b>	<b>9</b>
1.1 Motivation and objectives.....	9
1.2 Chapters summary.....	9
<b>2. Biological Background.....</b>	<b>10</b>
2.1 Pupil anatomy.....	10
2.1.1 Miosis.....	11
2.1.2 Pupil mobility.....	11
2.2 Physiology of the photomotor reflex.....	13
2.3 PLR and the autonomous nervous system.....	16
2.4 Beyond typical PLR.....	20
2.5 Clinical applications of pupillography.....	21
2.5.1 ANS Effects of phrmaceuticals.....	21
2.5.2 Psychiatric disorders.....	22
2.5.3 Brain and mental disorders.....	22
2.5.4 Diabetes and cardiovascular neuropathy.....	23
2.5.5 Alternative cures.....	24
2.5.6 Drugs, Alcohol.....	24
2.5.7 Cognitive state – awereness.....	24
<b>3. Materials and Methods.....</b>	<b>25</b>
3.1 Designing the Device.....	25
3.1.1 Scotopic measurement.....	25
3.1.2 Pupillary light reflex.....	26
3.1.3 Swinging flashlight test.....	28
3.1.4 Pupil control.....	29
3.1.5 Anisocoria.....	29
3.1.6 Software needs.....	30
3.2 Instrumentation.....	31
3.2.1 CCD Cameras.....	32
3.2.2 Infrared LEDs.....	35
3.2.3 White light LEDs.....	36
3.2.4 Microcontroller.....	38
3.2.5 Electrical Supply.....	39
3.2.6 Optical Filters.....	40
3.3 Mounting the device.....	40
3.4 Algorithm and Software Development.....	41
3.5 Acquisition method.....	48
3.6 Experimental setup.....	50
<b>4. Results &amp; Conclusions.....</b>	<b>51</b>

4.1 Subjects and methods.....	51
4.2 Pupillograms.....	51
4.3 Mathematical modeling and fitting.....	53
4.3.1 Definition of smoothing splines.....	55
4.3.2 Derivation of the smoothing splines.....	56
4.4 Interpretation of the results.....	60
4.4.1 Clinical studies pupillographic results.....	61
4.5 Discussion and conclusions.....	64
4.6 Future work.....	66
<b>References.....</b>	<b>67</b>
<b>List of abbreviations.....</b>	<b>69</b>
<b>Appendix.....</b>	<b>70</b>

## List of figures and charts

Figure 1 Anatomy of the human eye.....	11
Figure 2 Diagram of the pathways subserving pupillary light reflex.....	14
Figure 3 Reflex arc components.....	15
Figure 4 ANS side view.....	18
Figure 5 ANS front view.....	19
Figure 6 Brain pthways for pupil constriction and dilation.....	27
Figure 7 Swinging flashlight test practical examination.....	28
Figure 8 A schematic approach for sorting out the nature of anisocoria.....	31
Figure 9 PGR Dragonfly2.....	32
Figure 10 Arduino Diecimilla board.....	38
Figure 11 Image acquisition without IR band pass filter.....	40
Figure 12 Signal flow diagram.....	42
Figure 13 Parameter space used for circular HT.....	43
Figure 14 Finding the analytical form of a circle by an inscribed triangle.....	45
Figure 15 Three point Algorithm.....	46
Figure 16 Semi-closed eyes where the algorithm was successful.....	47
Figure 17 White spot on pupil's contour.....	47
Figure 18 All steps of a PLR test followed by the P.R.I.M.A. system.....	49
Figure 19 Prototype model.....	50
Figure 20 Demonstration of a test performance.....	50
Figure 21 Demonstration Result Set 1 .....	52
Figure 22 Demonstration Result Set 2.....	52
Figure 23 Calculating the first derivative through finite differences.....	54
Figure 24 Gaussian fitting on a pupillogram (unsuccessful).....	54
Figure 25 Curve fitting and derivation on.....	58
Figure 26 Curve fitting and derivation on.....	59
Figure 27 Pupillography curve fitting and derivation examples.....	60
Figure 28 Defect Pupillogram 1.....	61
Figure 29 Defect Pupillogram 2.....	62
Figure 30 Defect Pupillogram 3.....	63

## List of charts

Chart 1 Summary of Autonomous nervous systems responsibilities.....	18
Chart 2 Technical Characteristics of PGR DR-2 camera.....	34
Chart 3 Technical characteristics of the infrared LED.....	36
Chart 4 Technical characteristics of the white light LED.....	37
Chart 5 Technical specifications of Arduino Diecimilla microcontroller.....	39
Chart 6 Pupil's velocity and acceleration values on specific frames.....	58
Chart 7 Pupil's velocity and acceleration values on specific frames.....	59

# **1. Introduction**

## **1.1 Motivation and Objectives**

This study was conducted for two basic reasons. Firstly, to gain “hands on” experience on realistic applications of the knowledge provided throughout the undergraduate studies. Secondly, to research the current scientific progress on a specific field and attempt to improve it. This study belongs to the very demanding and challenging field of biomedical engineering. It is its purpose therefore to combine knowledge of various academic disciplines and scientific backgrounds for the shale of humanity, health improvement and welfare of people.

The objective of this project is the creation of a device that will be able to test the pupillary reflexes under several circumstances with high accuracy. The pupil is the most outer neural sensory receptor and it is regarded as the “brain’s gate”. However testing pupillary responses is an everyday part of clinical examination, but stays only at a superficial level. As recent surveys show, pupillary reflexes consist a window to the nervous system functionality. Their test is non-invasive, real-time and sensitive. The sensitivity though, is not perceptible by a human examiner and specialized instrumentation needs to be constructed.

This device is intended to serve as a novel diagnostic mean for the functionality of the nervous system, complying with the doctors’ adage “prevention is of higher importance than treatment”. Furthermore, it is designed with the long-term perspective of evaluating the cognitive and sentimental awareness of people. Pupillary reflexes examination, according to recent clinical studies, looks very promising for the near future of medical diagnosis means.

## **1.2 Chapters summary**

The chapters follow the steps that led to the design of this prototype device. In chapter 1 is provided the basic physiology knowledge of the anatomy of the human eye, the pupillary reflexes and the autonomous nervous system which regulates the reflex. Also the value of the PLR tests is discussed, through clinical applications results.

In Chapter 2 is described the instrumentation and the custom software development for this application, as well as the mounting and communication between the components. The clinical tests are described briefly, which guided the designing process.

All results and mathematical modeling of the resulting pupillogram are presented in chapter 3. Clinical surveys examples are shown in order to examine ways of evaluating the results.

## **2. Biological background**

### **2.1 Pupil anatomy**

The pupil is the sphere that is located in the center of the iris of the eye and that controls the amount of light that enters the eye (figure). It appears black because most of the light entering the pupil is absorbed by the tissues inside the eye. In optical terms, the anatomical pupil is the eye's aperture and the iris is the aperture stop. The image of the pupil as seen from outside the eye is the entrance pupil, which does not exactly correspond to the location and size of the physical pupil because it is magnified by the cornea. On the inner edge lies a prominent structure, the collarette, marking the junction of the embryonic pupillary membrane covering the embryonic pupil.

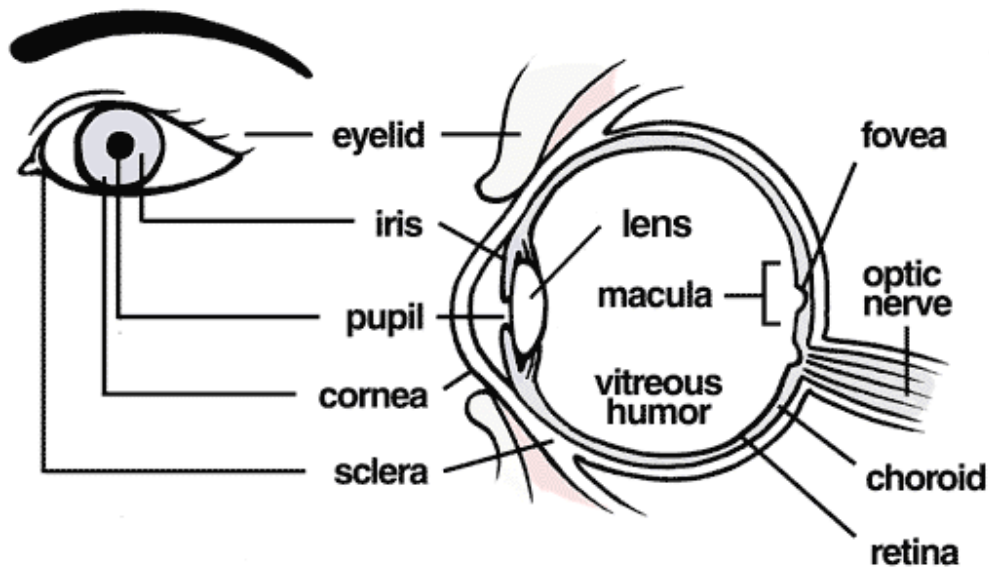


*Figure 1 Anatomy of the human eye*

### **2.1.1 Miosis**

Miosis is the constriction of the pupil of human eye. This is a normal response to an increase in light but can also be associated with certain pathological conditions, microwave radiation exposure and certain drugs. The opposite, mydriasis, is the dilation of the pupil. In the case of constriction due to light exposure, the reaction is named pupillary light reflex or photomotor reflex. This process implies the transformation of a photoelectrical phenomenon to a photochemical inside the brain.

### **2.1.2 Pupil mobility**

The testing of pupillary size and reactivity, which can be accomplished by the use of a flashlight, yields important, often vital clinical information. Essential, of course, is the proper interpretation of the pupillary reactions, and this requires some knowledge

of their underlying neural mechanisms. The diameter of the pupil is determined by the balance of innervation between the autonomically innervated sphincter and radially arranged dilator muscles of the iris, the sphincter muscle playing the major role. The pupilloconstrictor (parasympathetic) fibers arise in the Edinger-Westphal nucleus in the high midbrain, join the third cranial (oculomotor) nerve, and synapse in the ciliary ganglion, which lies in the posterior part of the orbit. The postganglionic fibers then enter the globe via the short ciliary nerves; approximately 3 percent of the fibers innervate the sphincter pupillae and 97 percent the ciliary body. The sphincter of the pupil comprises 50 motor units, according to Corbett and Thompson. The pupillodilator (sympathetic) fibers arise in the posterolateral part of the hypothalamus and descend, uncrossed, in the lateral tegmentum of the midbrain, pons, medulla, and cervical spinal cord to the eighth cervical and first and second thoracic segments, where they synapse with the lateral

horn cells. The latter cells give rise to preganglionic fibers, most of which leave the cord by the second ventral thoracic root and proceed through the stellate ganglion to synapse in the superior cervical ganglion. The postganglionic fibers course along the internal

carotid artery and traverse the cavernous sinus, where they join the first division of the trigeminal nerve, finally reaching the eye as the long ciliary nerve that innervates the dilator muscle of the iris. Some of the postganglionic sympathetic fibers also innervate

the sweat glands and arterioles of the face and Müller's muscle in the eyelid.

Generally the pupils do not remain completely still, therefore may lead to oscillation, which may intensify and become known as hippus. When only one eye is stimulated, both eyes contract equally. The constriction of the pupil and near vision are closely tied. In bright light, the pupils constrict to prevent aberrations of light rays and thus attain their expected acuity; in the dark this is not necessary, so it is chiefly concerned with admitting sufficient light into the

eye. The pupil dilates in extreme psychical situations (e.g., fear) or contact of a sensory nerve, such as pain.

It has been determined that every nerve supply has an inhibitor, and the eye is no exception. The sphincter muscle has a sympathetic antagonist supply, and the dilator has a parasympathetic (cholinergic) inhibitor. In pupillary constriction induced by pilocarpine, not only is the sphincter nerve supply activated but that of the dilator is inhibited. The reverse is true, so control of pupil size is controlled by differences in contraction intensity of each muscle.

Certain drugs cause constriction of the pupils, such as alcohol and opioids. Other drugs, such as atropine, marijuana, LSD, mescaline, psilocybin mushrooms, cocaine and amphetamines cause pupil dilation.

## **2.2 Physiology of the photomotor reflex**

A reflex is an automatic involuntary motor response to a stimuli. Specifically, for the photomotor reflex, as light entering the eye strikes three different photoreceptors in the retina: the familiar rods and cones used in image-forming and the more newly discovered photosensitive ganglion cells. The ganglion cells give information about ambient light levels, and react sluggishly compared to the rods and cones. Signals from ganglion cells have three functions: acute suppression of the hormone melatonin, entrainment of the body's circadian rhythms and regulation of the size of the pupil.

The retinal photoceptors convert light stimuli into electric impulses. Nerves pertaining to the resizing of the pupil connect to the pretectal nucleus of the high midbrain, bypassing the lateral geniculate nucleus and the primary visual cortex. From the pretectal nucleus neurons send axons to neurons of the Edinger-Westphal nucleus whose visceromotor axons run along both the left and right

oculomotor nerves. Visceromotor nerve axons (which constitute a portion of cranial nerve III, along with the somatomotor portion derived from the Edinger-Westphal nucleus) synapse on ciliary ganglion neurons, whose parasympathetic axons innervate the constrictor muscle of the iris, producing miosis. This occurs because sympathetic activity from the ciliary ganglion is lost thus parasympathetics are not inhibited.

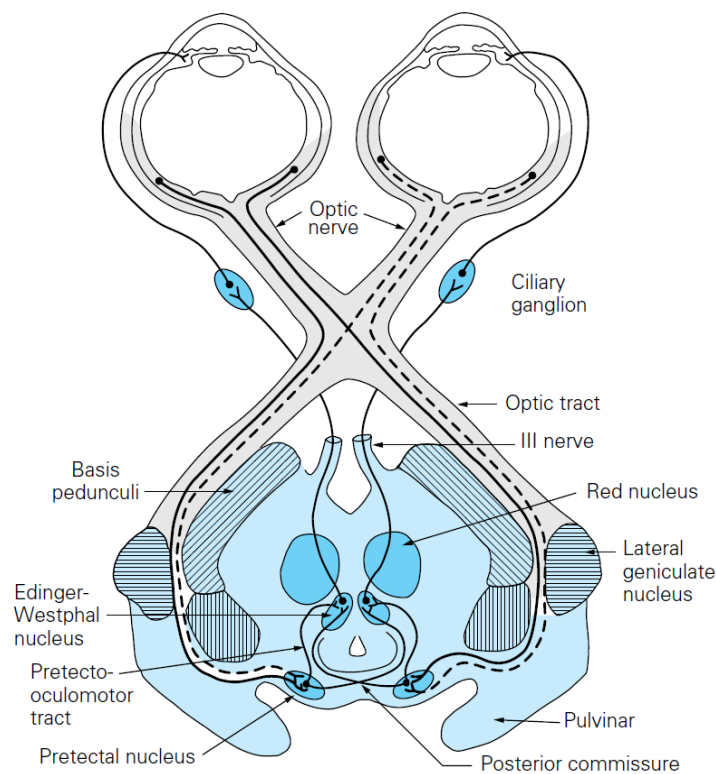


*Figure 2. Diagram of the pathways subserving the pupillary light reflex.*

On the above diagram, the three parts of PLR pathway can be seen:

1. An afferent limb, whose fibers originate in the retinal receptor cells, pass through the bipolar cells, and synapse with the retinal ganglion cells; axons of these cells run in the optic nerve and tract. The light reflex fibers leave the optic

tract just rostral to the lateral geniculate body and enter the high midbrain, where they synapse in the pretectal nucleus.

2. Intercalated neurons that give rise to the pupillomotor fibers, which pass ventrally to the ipsilateral Edinger-Westphal nucleus and, via fibers that cross in the posterior commissure, to the contralateral Edinger-Westphal nucleus (labeled “pretecto-oculomotor” tract in Fig. 14-7).

3. An efferent two-neuron pathway from the Edinger-Westphal nucleus, synapsing in the ciliary ganglion, by which all motor impulses reach the pupillary sphincter, as described above.

All the reflexes in human body follow a reflex arc, structured with five components.

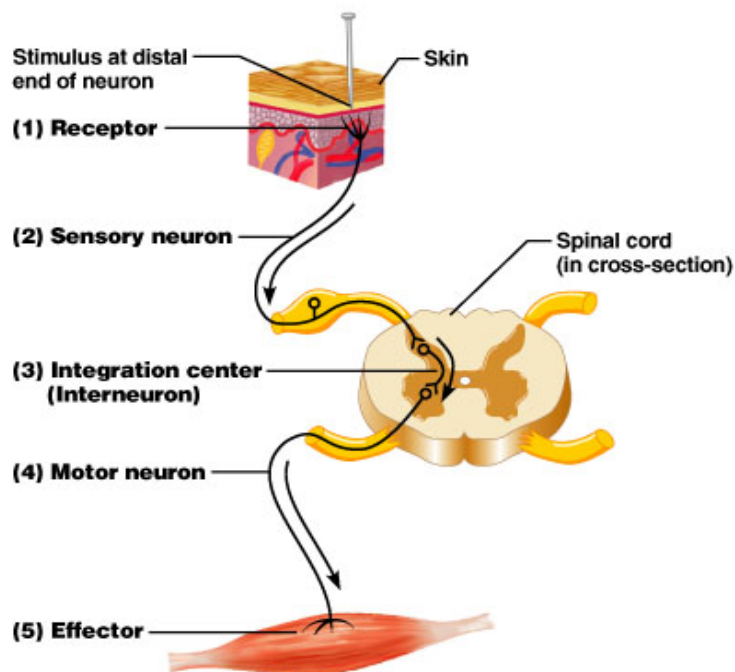


*Figure 3 Five components to the reflex arc*

## 2.3 PLR and the Autonomous Nervous System

The **Pupillary Light Reflex (PLR)** is a reflex that controls the diameter of the pupil, in response to the intensity (luminance) of light that falls on the retina of the eye. Greater intensity light causes the pupil to become smaller, allowing less light in, whereas lower intensity light causes the pupil to become larger, allowing more light in. Thus, the pupillary light reflex regulates the intensity of light entering the eye. This reflex is controlled by the **Autonomous Nervous System (ANS)**.

The autonomic nervous system, or visceral nervous system, is the part of the peripheral nervous system that acts as a control system, maintaining homeostasis in the body. It regulates the sequence of basic physiological events allowing an organism to optimally adjust to environmental changes. These activities are generally performed without conscious control. The ANS affects heart rate, digestion, respiration rate, salivation, perspiration, diameter of the pupils, micturition (urination), and sexual arousal. Whereas most of its actions are involuntary, some, such as breathing, work in tandem with the conscious mind.

The ANS influences every cell in the body through its two branches: the sympathetic nervous system (sympathetics - SNS) and the parasympathetic nervous system (parasympathetics - PNS). In general, the sympathetics are responsible for mediating energy expenditure, while the parasympathetics are responsible for energy conservation and restoration. For example, the sympathetics mediate the "fight or flight" response and the body's response to stress, pain, and cold. Thus, the sympathetics cause higher heart rates and respiratory rates, shunting blood from the extremities to core organs and muscles (e.g., running or shivering), etc. Both PNS and SNS are under the regulatory of upper centers, particularly the anterior and posterior hypothalamus.

The parasympathetics mediate resting states after meals and at night, digestion and nutrient storage, and recovery states by helping to coordinate immune responses and healing. Thus, the parasympathetics cause slower heart rates and respiratory rates, sleep, increased gastrointestinal track motility, increased peripheral vascular flow, blood flow to all cells, liver and kidneys, and venous return to the heart. The sympathetic and parasympathetic branches of the ANS work together to maintain homeostasis.

When the ANS affects a change in the body (e.g., heart rate or respiratory rate), it works only to cause the change. The ANS then returns to its baseline state. So, periodic excursions in one or the other branch from baseline are normal and expected as long as the ANS returns to baseline in a timely manner. Persistently elevated levels of tone in one or the other branch are not healthy.

The general action of each of the branches of the ANS is to oppose the other. As one branch begins to work the other branch begins to return it to baseline. Consequently, persistently elevated tone in one branch can result in a persistently depressed tone in the other. This only serves to compound an unhealthy situation. So, balance between the branches is as important as overall tone in each of the branches.

It has been learned that the parasympathetic nervous system can change faster than the sympathetic nervous system. Thus, as the sympathetics start to mediate a stress response the parasympathetics immediately begin to counter it. If the parasympathetics were not faster than the sympathetics, then any stress response could send the heart into tachycardia and onto ventricular fibrillation before the parasympathetics could act to prevent it. The parasympathetics, through the Vagus, are the main controlling influence on respiratory activity. Increases in respiratory analysis are caused by increases in parasympathetic tone. Parasympathetic input to the heart is through fibers that synapse deep in the myocardium. Sympathetic influence on the heart is through surface

synapses. Due to this arrangement the parasympathetics are more sensitive to heart damage (i.e., infarct, ischemia, or cardiomyopathies). Since the parasympathetics are faster to respond, it is usually the branch that is first to indicate changes in health status anywhere in the body.

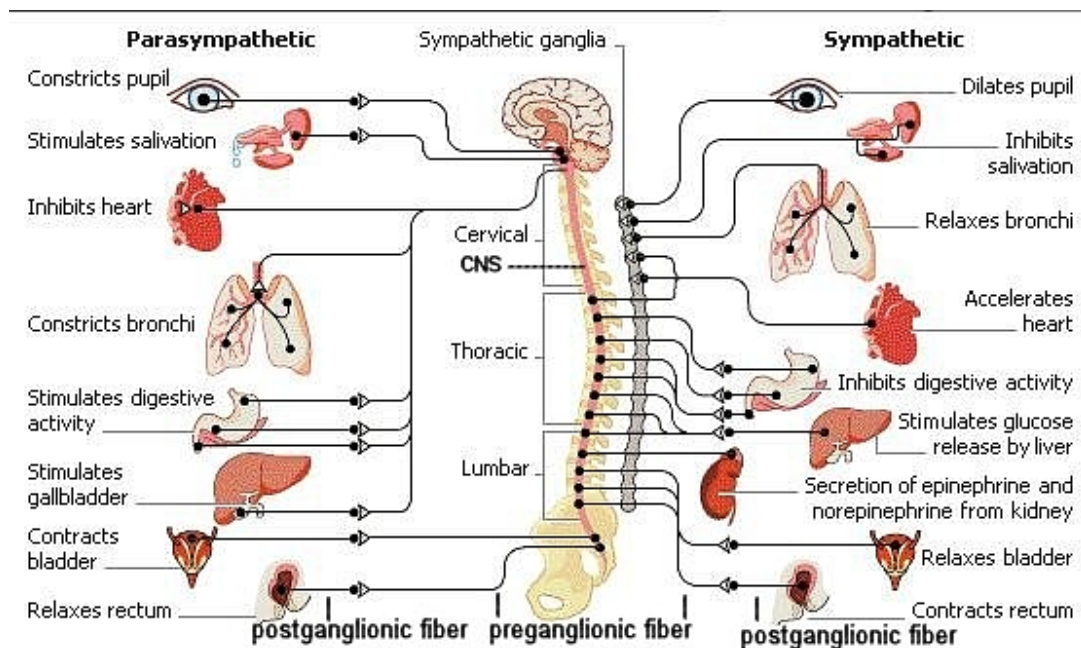


Figure 4 ANS side view

### Autonomic Nervous System targets

Organ	Sympathetic role	Parasympathetic role
Eye	Dilates pupil	Constricts pupil
Salivary glands	Dry mouth (thick saliva)	Lots of dilute saliva
Heart rate	Increases	Decreases
Lungs (bronchi)	Dilates	Constricts
GI activity	Decreases	Increases
Liver	Increases blood sugar	None
Adrenal medulla	Stimulates secretion	None
Penis	Ejaculation	Erection

Chart 1 Summary of ANS responsibilities in human body

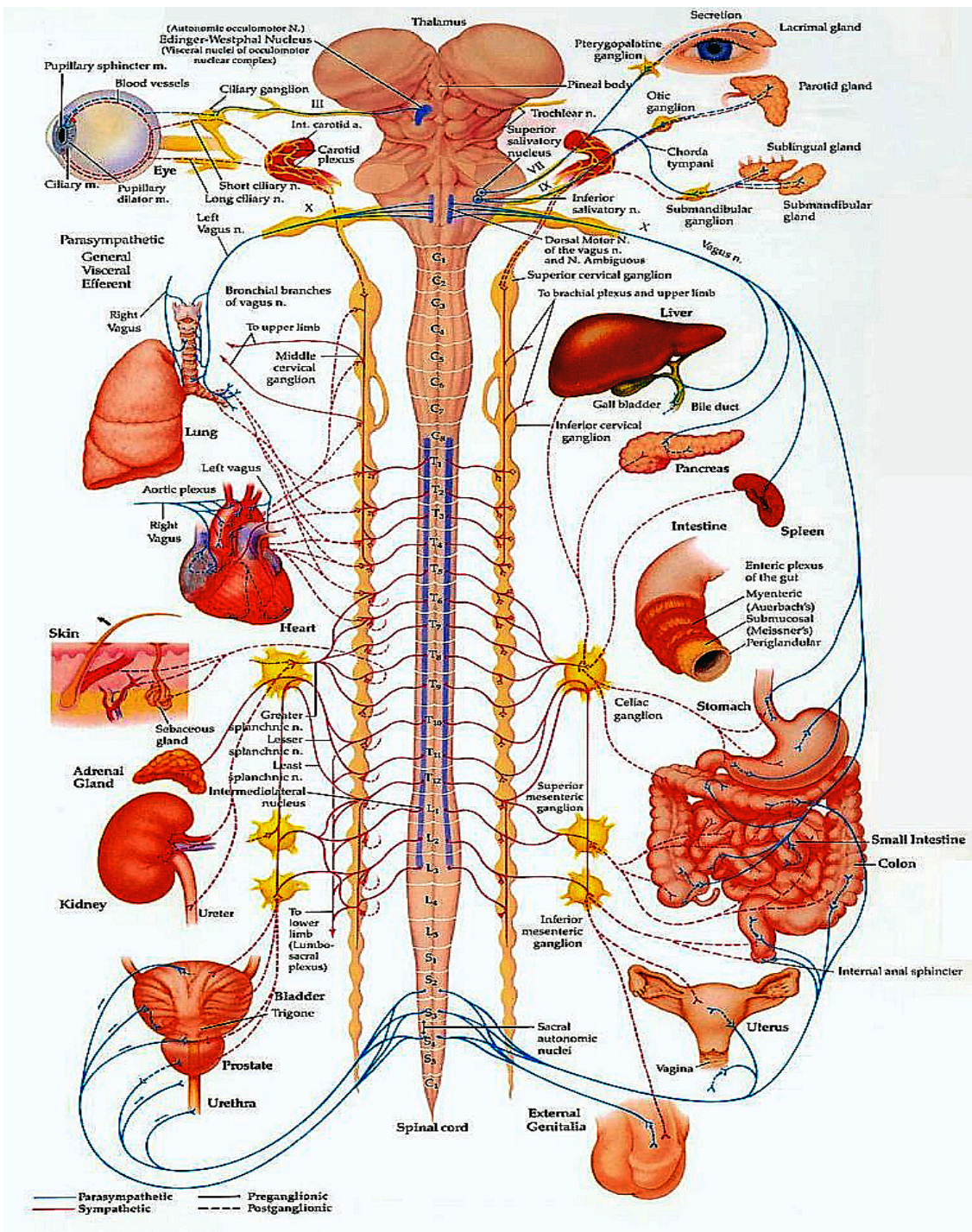


Figure 5 ANS front view

## 2.4 Beyond typical PLR

Pupil's reaction to light presents a window to the sympathetic and parasympathetic nervous system and is a part of every clinical neurophysiological examination. Despite the popularity, it remains underestimated. It is used mostly to check the existence of the reflex (direct and indirect) and the speed, using subjective criteria. Although various recent clinical surveys have shown that pupillometry may be far more valuable as a diagnostic mean. These applications will be discussed shortly. For this purpose although, the abilities of a clinical doctor using a penlight are inadequate.

The mobility of the pupil is fast, variable and non linear. In a typical PLR examination it is estimated that maximum constriction will occur in less than one second and the diameters are in the range of millimeters. These factors exceed human perception abilities and thus, specific instrumentation needs to be constructed, able of measuring both diameter and speed with accuracy. Computerized pupillography has the following important advantages [1]:

1. Measurements can be performed more accurately.
2. Additional parameters can be measured, such as pupil latency time.
3. Findings can be documented and compared from examination to examination.
4. Observations are not influenced by examiner bias.
5. Normal values can be established to distinguish more clearly between pathologic and normal findings.

6. New information about pupil behavior can be obtained, which allows a better understanding of physiology and pathophysiology.

The last decade a new experimental technique has been developed, known as infrared pupillometry. This term implies the use of electronic mediums for capturing and processing pupil images under the circumstances of various tests. Devices have been developed and may be found as publications, patents or in the market. The goal of project PRIMA is the study of all devices, the research of the hidden information behind the pupillary responses and the mounting of a new clinical testing device which is able to exploit pupillometry deeply as clinical examination.

## **2.5 Clinical applications of Pupillography**

Different neuroanatomical pathways are involved in pupil control and their neurological integrity and functionality can be often ascertained through the analysis and interpretation of the pupil behavior. This makes the pupil an important element to be analyzed in many clinical procedures. Here follows a brief statement of clinical applications of pupillography and recent surveys.

### **2.5.1 ANS Effects of Pharmaceuticals**

Any drug that acts on the central nervous system affects the pupillogram. For most substances, it is difficult to predict which arm of the autonomous nervous system will be most influenced [2]. Pupil dilation can be observed after either parasympatholytic or sympathomimetic drugs, and pupil constriction after parasympathomimetics or sympatholytics. The pupillogram provides sensitive information on cholinergic or adrenergic effects. The latency of the pupillary light reflex is predominantly regulated by the parasympathetic system; the dilation speed best

reflects the action of the sympathetic system. By blocking the dilator muscle with dapiprazole eye drops, one can determine whether pupil dilation is caused by central inhibition of cholinergic activity. Additionally, by applying the pupillographic sleepiness test, sedative effects of a drug can be assessed objectively [2].

### **2.5.2 Psychiatric disorders**

Pupillography has also been used to objectively measure emotional responses. Fear, anger or stress, dilate the pupil, an effect called the “psychosensory pupillary response”. Psychosensory pupil dilation is often less than 0.3 mm, and can be hidden within the normal, spontaneous oscillations of pupil size, which are of the same magnitude. Therefore, pupillography is necessary to isolate the psychosensory response, mostly by averaging several response reflexes similar to what is done to extract the Visual Evoked Potential (VEP) from the Electroencephalography (EEG) recording. Patients with different psychiatric disorders will display different emotional reactions to stimuli presented to them [3]. For example, an alcoholic patient will react differently to the smell of whisky if this patient is a recidivist risk after withdrawal therapy. Pupillographic data exist in a great number of psychiatric patients, but the data have not been sufficiently confirmed to allow their clinical application. However, the use of pupillography in psychiatric disorders is promising.

### **2.5.3 Brain and Mental Disorders**

Brain and mental diseases unfortunately affect more and more people during the last decades and it is estimated that this is going to maintain an anabatic course. Early diagnosis and prediction are of vital importance for the avoidance of severe phenotype. Today, in some cases like Alzheimer, they can accurately and definitely 100% be diagnosed only by histological examination of brain tissue

obtained by biopsy or autopsy (post mortem). Until now, there is no early, non-invasive, sensitive and easily administered diagnostic method for the diagnosis of the above diseases. Clinical studies are relating PLR and pupil sensitivity with these neurophysiological diseases.

There are Pupillographic results in surveys which correlate pupil mobility (latency) with Alzheimer disease and Parkinson's syndrome [4], though they are still in a preliminary stadium and need to be reproduced. Another survey has shown that depressed individuals were especially slow to name the emotionality of positive information, and displayed greater sustained processing, expressed also by sustained pupil dilation (irrelative with the ambient illumination) [5]. Patients suffering from Schizophrenia are being studied in order to reveal the exact biophysical consequences of the disease [6]. Multiple sclerosis (encephalomyelitis disseminata), an autoimmune condition in which the immune system attacks the central nervous system, is studied along with the direct and consensual pupillary responses [7].

#### **2.5.4 Diabetes, Cardiovascular Neuropathy and Sexually transmitted diseases**

Apart from the afore mentioned diseases, there several others which affect the ANS, including abnormalities in metabolism in blood sugar level (Diabetes mellitus), heart failures (Cardiovascular neuropathy) [8] and venereal diseases (Tertiary syphilis and neurosyphilis). The effect on PLR is mentioned since decades, but this hasn't been examined thoroughly in order to elicit diagnostic or early stadium findings. Recent studies on pupillography are researching this field [9]. It is important to mention that in Diabetes Autonomous Neuropathy (DAN) pupillary autonomic dysfunction occurs before cardiovascular autonomic changes and detection of pupil denervation hypersensitivity through PLR is an inexpensive way to detect early DAN.

### **2.5.5 Alternative Cures**

In medical research, there is a sector which studies alternative and traditional curative methods. In some cases pupillary responses are included in the surveys for the study of ANS effects. In acupuncture, which has a wide treating field, the pupil is studied along with the effects of stimulating specific points on the human body and the position of the patient [10]. Chronic headaches are studied through Kampo, the Japanese study and adaptation of the traditional Chinese medicine. This type of disease has as an effect the autonomous nervous imbalance and thus, pupil reflexes study is a window for this. A cure by a traditional medicine called “goshuyuto” remedies the balance and this is obvious through PLR [11].

### **2.5.6 Drugs – Alcohol**

The effect of illegal drugs and alcohol on the central nervous system is known. The changes of the pupil reflexes and condition are also reported. PLR can function as a diagnostic mean to test the consumption of such substances [12]. It is ambiguous whether this tactic has a beneficial effect on the society in general. On the other hand, PLR is a reporter of the mental and emotional condition of a subject. This implies that any intense mental or sentimental arousal will be combined with a pupillary reflex. This observation may be very useful in cases of rehabilitation from the above substances, in a way of understanding whether the will of the person against them is honest and strong and how does he react to the idea of them in terms of his senses excitation (e.g. smell) to them, as it was stated in the psychiatric disorders.

### **2.5.7 Cognitive state, Awareness and Sleepiness**

Pupil reflexes and PLR are strongly connected with the cognitive load of a person, as well as with his awareness state. Pupillometry has served

psychophysiology in its studies of the dynamics of human cognitive processing, in particular using Task Evoked Pupillary Responses (TERPs). PLR combined with other autonomic nervous functions, such as cardiovascular measurements, provide a wide range study on mental and emotional of a person and has a rising research interest [13]. Also, as an awareness measure, may reveal sleepiness or fatigue.

*Pupillary responses are studied in many other areas as well, such the function of neurotransmitters and hormones, but there is no need for further discussion at this point.*

### **3. Materials & Methods**

#### **3.1 Designing the device**

The goal of this project is the creation of a device with the ability to record the diameter of the pupil under specific circumstances. These circumstances are defined by the types of medical tests which will be conducted. A closer study to the practical performance of these tests will reveal the needs and the specifications of the P.R.I.M.A. system.

##### **3.1.1 Scotopic measurement**

Scotopic measurement is done in absolute darkness, where the pupil reaches the maximum dilation and thus, maximum diameter. As it is supposed, infrared capturing is needed in order to detect the pupil and count its size.

This leads to the following engineering assumptions about the needs of the system:

- An infrared lighting source
- An infrared band capturing digital camera

### **3.1.2 Pupillary light reflex - PLR**

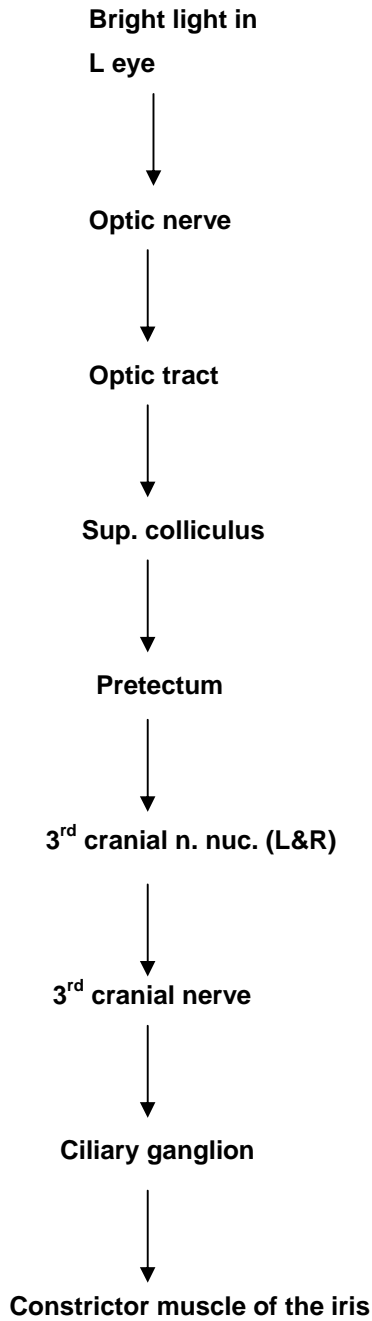
The PLR is performed by stimulating the eye with a light source, focusing on the pupil. The most common and widely used medium is a “pen torch”. The distance between the eye and the source is usually 10 to 15 cm (4 – 7 inches). From this distance the intensity light of the pen torch is adequate. There is a delay from the moment the light is on and the constriction of the pupil begins, because of the biological functions which transform a photoelectrical phenomenon to a photochemical inside the brain. This is usually referred as latency. Also when full constriction has occurred, the pupillary reaction becomes saturated and the stimulation should stop. For capturing the reaction, studies conclude that the video frame rate should be around 60 Hz and above.

This leads to the following engineering assumptions about the needs of the system:

- A digital camera with a high framerate to record the pupil changes
- A stimulation medium

The reflexes of constriction and dilation of the pupil are generally the parameters that in a pupillary reflex test are examined. The reflexes have latency as said previously and this time period must be measured precisely, in order to examine the function of the ANS. This occurs due to various biochemical processes inside human brain, which involve the following steps (through neurophysiological pathways) during PLR:

Constriction



Dilation

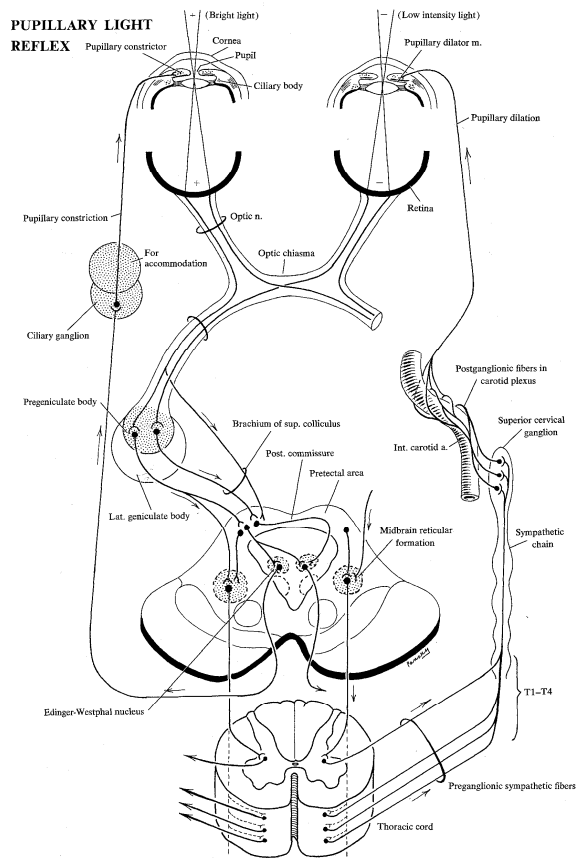
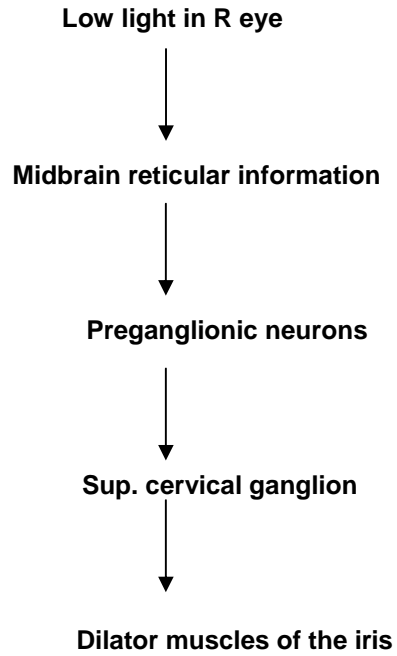
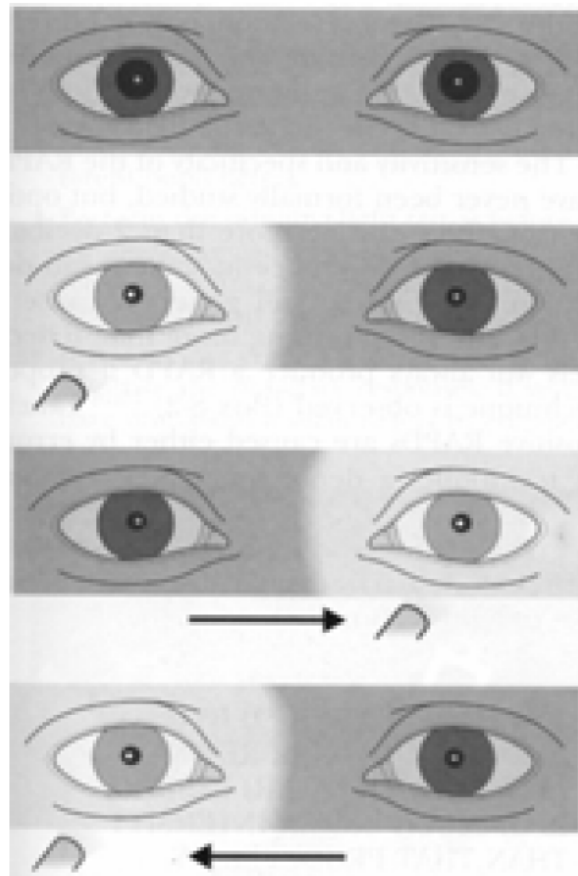


Figure 6 Brain pathways of pupil constriction and dilation

### 3.1.3 Swinging flashlight test

The swinging flashlight test is performed under near scotopic conditions. The examinee fixates on a distant target. The stimulation light should be directed to the eye in an angle of  $45^\circ$  to the optical axis from below to the upper peripheral retinal. The distance should be about the same as in PLR. The stimulation is performed for 2 – 4 sec for one eye and then there is a rapid swing to the other eye. The distance and the intensity must not change during the test [14]. The pupillary responses of both eyes are examined, meaning both direct and consensual reflexes.



*Figure 7 Swinging flashlight test practical examination*

This leads to the following engineering assumptions about the needs of the system:

- Two cameras, in order to record the consensual reflex
- Stimulation medium
- An automated signal control subsystem has to be created to synchronize illumination, stimulation and the cameras record

*This implementation is to be designed on future work; the investigation though is done from in this part.*

#### **3.1.4 Pupil control**

Another type of pupil non invasive examination tests is the control of the pupil size by low power adjustable illumination. When it is done manually, the performer moves the source slightly towards the eye and backwards, trying to synchronize with the examinee's pupil. This test is examining the near reflexes of the pupil and tries to control its size. Although it seems trivial as an examination, using fast pupillometry, the near reflexes can be measured accurately, providing useful information on the medical subjects discussed already but also on the visual acuity and adaptivity. Near reflexes are very sensitive and require sensitive measuring methods.

This leads to the following engineering assumptions about the needs of the system:

- An adjustable illumination source with variable intensity and a mechanical mechanism able of stimulating the eye from several angles

#### **3.1.5 Anisocoria and Relative afferent pupillary defect tests**

Anisocoria is a condition characterized by an unequal size of the pupils. In the absence of any deformities of the iris or eyeball proper, anisocoria is usually the result of a defect in efferent nervous pathways controlling the pupil traveling in the oculomotor nerve (parasympathetic fibers) or the sympathetic pathways. Physical lesions and drugs causing anisocoria will do so via disruption of these pathways. There are ANS causes of anisocoria and others, which include extra than only ANS parameters, such as the afferent pupillary defect. Also, 20% of people may have a non pathological anisocoria. So, an objective test must be conducted to diagnose the type. This is done through a “decision tree” as would said in Statistics, like the following one:

### **3.1.6 Software needs**

The system must be accompanied by a skillful and practical software application. Basically the software must be able to load the acquired pictures, process them, locate the pupil and calculate the diameter. The lateral, demands the design of an effective algorithm for digital image processing. This procedure concerns all cameras frames. Finally, having acquired the total evolution of the phenomenon, the data is being processed and the results are shown. The needs of the system do not demand real time processing, so the calculations may be done completely offline.

Having set up the device, according to the previous guidelines, the test of the nature of anisocoria would be a matter of software processing. The diagnosis may be conducted through a decision tree (figure 8).

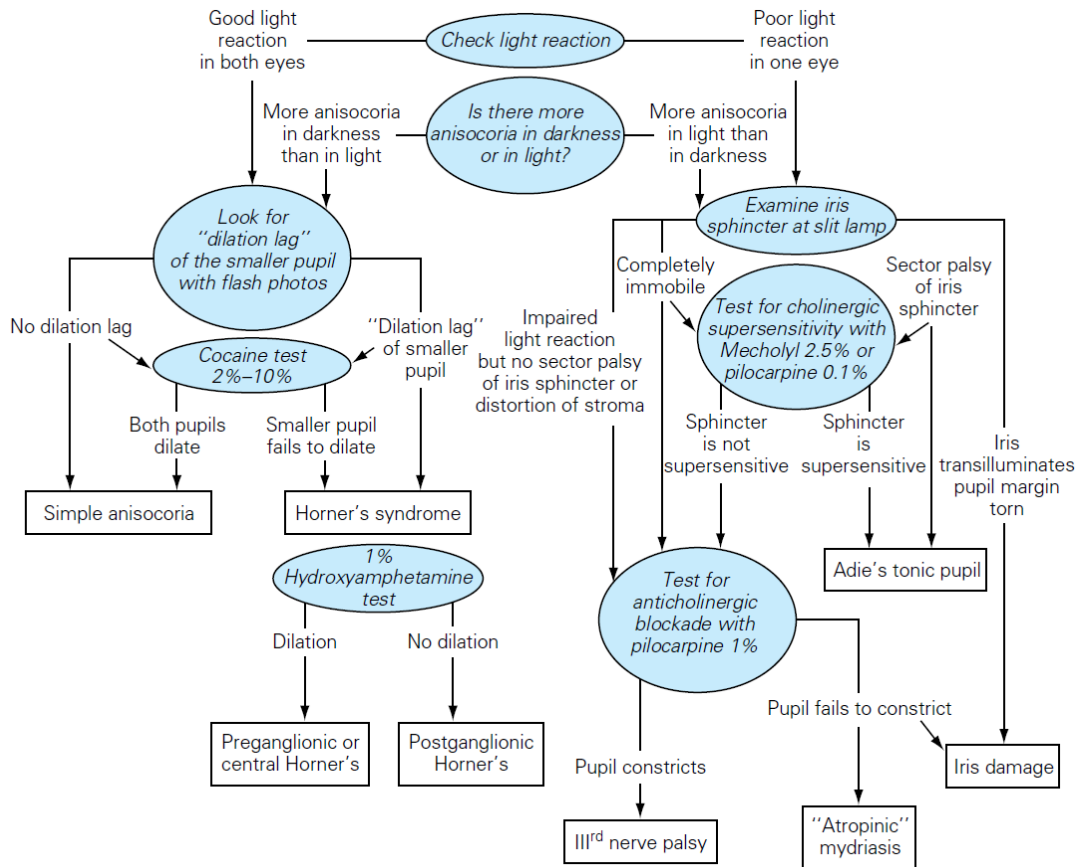


Figure 8 A schematic approach for sorting out the nature of anisocoria

### 3.2 Instrumentation

Taking into consideration all the above engineering assumptions, conclusively, the following instrumentation was selected as hardware components of the system.

1. CCD cameras 60fps – one for each eye
2. Infrared LEDs for illumination
3. White light LEDs for stimulation
4. Microcontroller for time, frequency and intensity synchronization
5. Electrical supply

## 6. Optical filters

### 3.2.1 CCD Cameras

The CCD camera for this implementation was the POINT GREY Dragonfly2 DR-2 Model. There are various reasons for selecting this model and manufacturer. Its features, which will be discussed next, cover the project needs fully and also PGR provides the camera with adequate documentation and with a Software Development Kit (SDK).

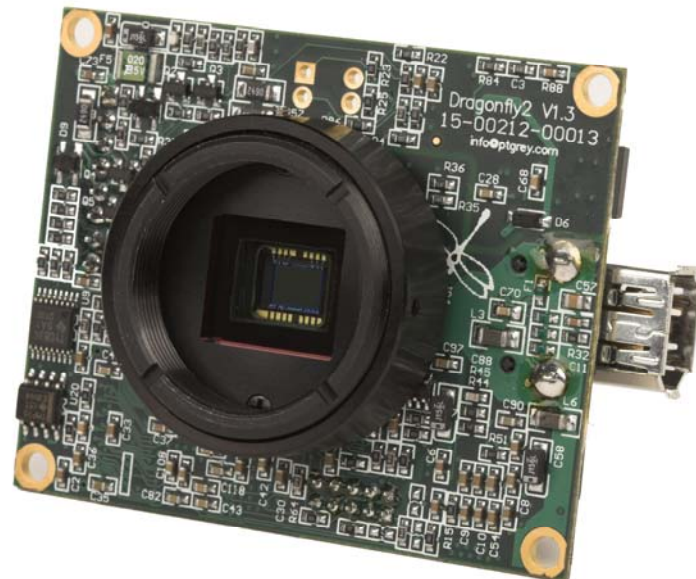


Figure 9 PGR Dragonfly2

The most important features of the camera are the following:

#### *Image Acquisition*

- 12-bit analog-to-digital converter
- Multiple cameras on the same 1394 bus automatically sync
- Faster standard frame rates, pixel binning and ROI
- Bulb-trigger mode, multiple triggered exposures before readout

- Overlapped trigger input, image acquisition and transfer

### *Image Processing*

- On-camera conversion to YUV411, YUV422 and RGB formats
- On-camera control of sharpness, hue, saturation, gamma
- Horizontal image flip (mirror image)
- Continuous static image for testing and development
- Pixels contain frame-specific info (e.g. 1394 cycle time)

### *Camera and Device Control*

- Broadcast settings to all cameras on the same bus
- On-board DC output for use by an auto iris lens
- Auto and one-push white balance for easy color balancing
- Reports the temperature near the imaging sensor
- Monitors sensor voltages to ensure optimal image quality
- Fine-tune frame rates for video conversion (e.g. PAL, NTSC)
- Non-volatile storage of camera default settings and user data
- Configurable strobe pattern output
- General purpose input/output pins for external device control
- Provides serial communication via GPIO digital logic levels
- Firmware upgradeable in field via IEEE-1394 interface.

### **Camera specifications**

Overview	OEM board-level camera
Imaging Sensor	Sony 1/3" progressive scan CCD
Sensor Size	Diagonal 6mm
Sensor Active Pixels	640(H) x 480(V)

Sensor Chip Size	5.79mm(H) x 4.89mm(V)
Sensor Unit Cell Size	7.4um(H) x 7.4um(V)
A/D Converter	Analog Devices 12-bit A/D converter
Video Data Output	8 and 16-bit digital data
Standard Resolutions	640x480, 320x240, 160x120
Frame Rates	60, 30, 15, 7.5, 3.75, 1.875 fps
Partial Image Modes	Pixel binning and region of interest modes
Interfaces	6-pin IEEE-1394 for camera control and video data transmission 4 general purpose digital input/output (GPIO) pins
Voltage Requirements	8-32V via IEEE-1394 cable or GPIO connector
Power Consumption	Less than 2W
Gain	Automatic/Manual/One-Push Gain modes 0dB to 24dB
Shutter	Automatic/Manual/One-Push Shutter modes 0.01ms to 66.63ms @ 15fps Extended Shutter modes 0.01ms to 7900ms @ 15fps
Gamma	0.50 to 4.00
Trigger Modes	DCAM v1.31 Trigger Modes
Signal to Noise Ratio	Greater than 60dB
Dimensions	63.5mm x 50.8mm x 13.15mm (bare board)
Mass	25 grams (bare board)
Camera Specification	IIDC 1394-based Digital Camera Specification v1.31
Emission Compliance	Complies with CE rules and Part 15 class A of FCC rules
Operating Temperature	Commercial grade electronics rated from 0 – 45 C
Storage Temperature	-30°C to -60°C
Operative Relative Humidity	20 to 80 % (no condensation)
Storage Relative Humidity	20 to 95 % (no condensation)
Current Firmware Version	0.9 Release Candidate 30

*Chart 2 Technical Characteristics of PGR DR-2 camera*

The programming language used for the communication between a personal computer and the camera was C++. This involves capturing and signaling, through the General Purpose Input Output (GPIO) pins of the camera. The lens that was used was a 25mm F/1.4 type with an extra spacer.

### 3.2.2 Infrared LEDs

A high speed infrared emitting diode, 870 nm, GaAlAs Double Hetero was used, model TSHA4401 of Vishay Semiconductors.

	<p><b>Description</b></p> <ul style="list-style-type: none"><li>• IR EMITTER, 3MM, 875NM</li><li>• Wavelength, typ:875nm</li><li>• Power dissipation:180mW</li><li>• Current, forward If:100mA</li><li>• Voltage, Vf max:1.5V</li><li>• Angle, viewing:40°</li><li>• Case style:Radial</li><li>• Temperature, operating range:-55°C to +100°C</li><li>• Angle, half:20°</li><li>• Current, If av:100mA</li><li>• LED / lamp size:3mm/T1</li><li>• Pitch:1.27mm</li><li>• Radiant intensity:60mW/Sr</li><li>• Radiant intensity, max:30mW/Sr</li><li>• Radiant intensity, min:16mW/Sr</li></ul>
---	--

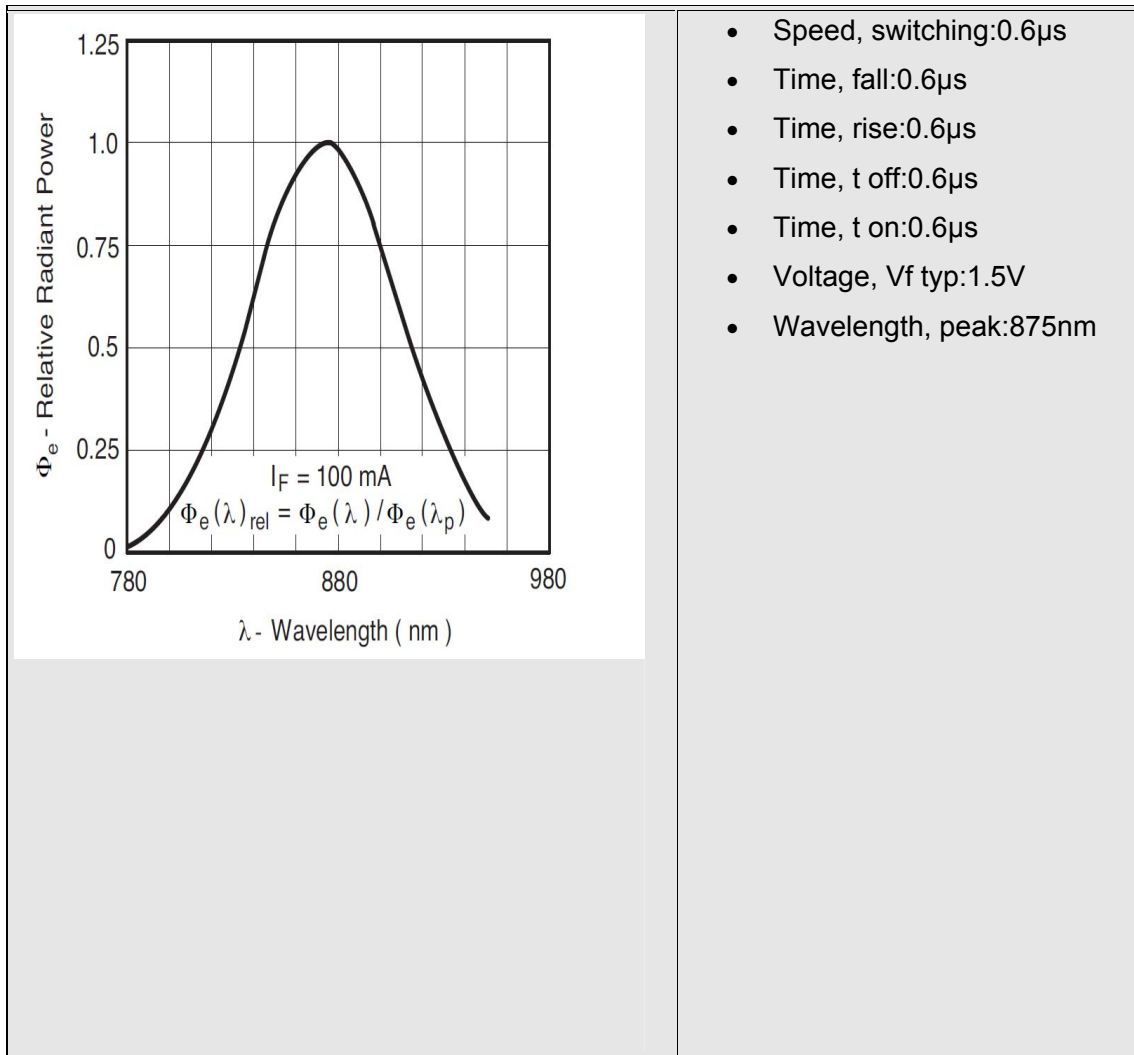


Chart 3 Technical characteristics of the infrared LED

### 3.2.3 White Light LEDs

High Intensity LED with typical color coordinates  $x = 0.33$ ,  $y = 0.33$  (typical color temperature 5500 k). This LED emits white light with a high color rendering index. It is the model VLHW4900 of Vishay Semiconductors.



## Description

- LED, 3MM, WHITE
- LED / lamp size:3mm
- Colour, LED:White
- Angle, viewing:32°
- Voltage, Vf max:4.2V
- Temperature, operating range:-40°C to +100°C
- Angle, half:16°
- Case style:T 1
- Colour temperature, typ:5500K
- Colour, lens:Water Clear
- Current, If max:30mA
- Current, forward If:20mA
- Diameter, External:3.2mm
- Diameter, head:3mm
- Length / Height, external:5.5mm
- Length, lead:24.8mm
- Luminous intensity, min:240mcd
- Luminous intensity, typ:500mcd
- Material:InGaN TAG on SiC
- Pitch, lead:2.54mm
- Power dissipation:126mW
- Temp, op. max:100°C
- Temp, op. min:-40°C
- Temperature, storage max:100°C
- Temperature, storage min:-40°C
- Voltage, PIV max:5V
- Voltage, Vf typ:3.5V

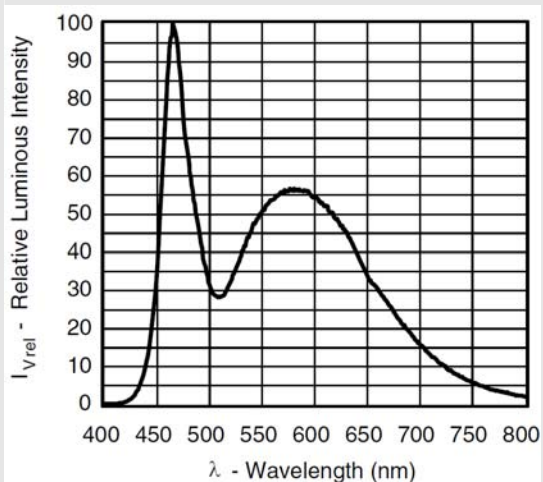
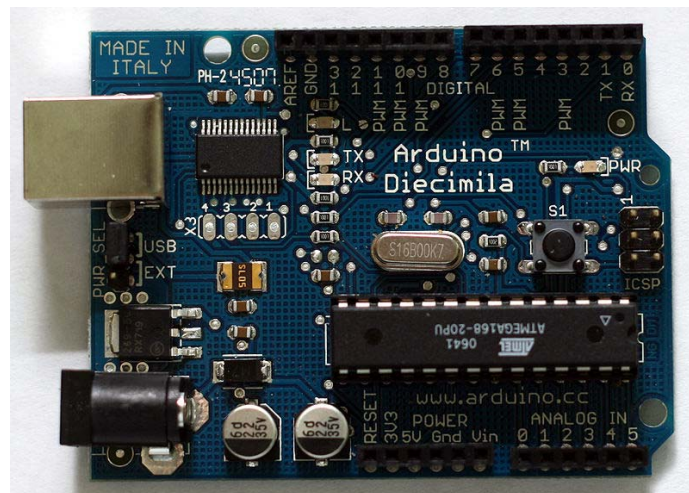


Chart 4 Technical characteristics of the white light LED

### 3.2.4. Microcontroller

A microcontroller is needed to govern and synchronize all the signals of the system. In this case, the signals are actually TTL pulses which do not carry data. Their goal is to enable or disable certain components (ON - OFF). Thus, a common microcontroller is needed.

The model used is the Atmel AVR ATmega168, 8-bit microcontroller, which covers the needs sufficiently. The microcontroller was mounted and preassembled on a board called Arduino Diecimilla. An Arduino board also consists of complementary components to facilitate programming and incorporation into other circuits. The board includes a 5-volt linear regulator and a 16MHz crystal oscillator. The microcontroller is pre-programmed with a bootloader so that an external programmer is not necessary. The interface with the computer is done through USB connection, which is downgraded to USB-to-serial, and supportive adapter chips on the board.



*Figure 10 Arduino Diecimilla board*

The Arduino IDE is a cross-platform Java application that serves as a code editor and compiler and is also capable of transferring firmware serially to the board. The development environment is based on the language “Processing”. The

programming language is derived from Wiring, a C-like language that provides similar functionality.

By using such a microcontroller, apart from the ease on programming it, there is extra safety for the hardware. The supportive circuits of the board protect the chip and other components connected or supplied by the microcontroller, from steep momentary changes on the potential difference, such as a voltage drop.

<b>Technical Specifications</b>	
Microcontroller	ATmega168
Operating Voltage	5V
Input Voltage (recommended)	7-12 V
Input Voltage (limits)	6-20 V
Digital I/O Pins	<b>14</b> (of which 6 provide PWM output)
Analog Input Pins	<b>6</b>
DC Current per I/O Pin	40 mA
DC Current for 3.3V Pin	50 mA
Flash Memory	16 KB (of which 2 KB used by bootloader)
SRAM	1 KB
EEPROM	512 bytes
Clock Speed	16 MHz

Chart 5 Technical specifications of Arduino Diecimilla microcontroller

### **3.2.5 Electrical Supply**

At this point, where the device is not yet portable, there is not one main unit which supplies the system with energy. The camera and the microcontroller are powered by the 1394 Firewire and the USB cable respectively. The LEDs are powered by the microcontroller that provides sufficient current for them.

### 3.2.6 Optical Filters

There are 2 types of optical filters used in the system. An IR band-pass filter and a polarizer. The IR band-pass filter allows only infrared light to come through and it is placed in front the lens. This suggests that the IR light LEDs will be always ON during the tests. The benefits of this optical setup are very important, because white light flashes do not distort the images and the intensity of grey levels is stable throughout the tests.

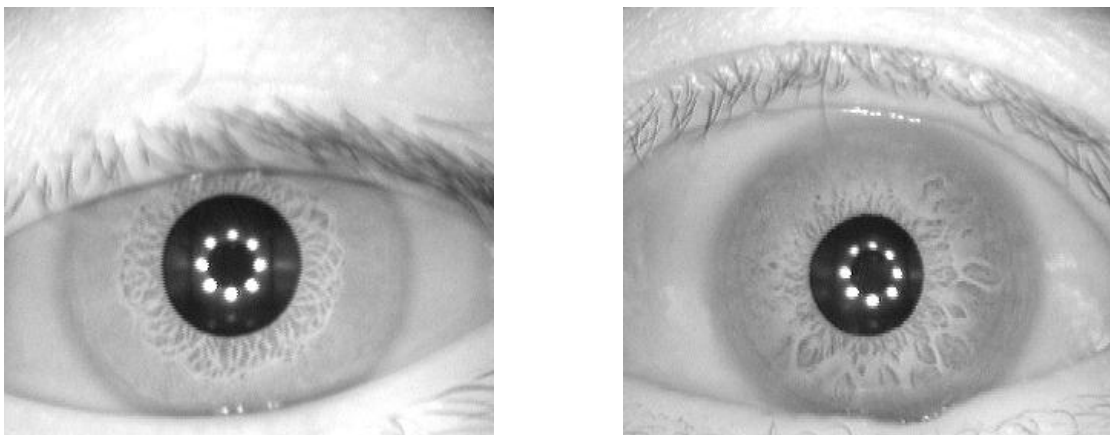


*Figure 11 Image acquisition without IR band pass filter*

### 3.3 Mounting the device

To mount the device, apart from the correct values of voltage and current for each electronic element of the device, the synchronization and the communication between the components must be assured as well.

#### *Powering each component*

The camera and the microcontroller are powered via the Firewire and the USB cable respectively. The LEDs are powered through the microcontroller. Each output of it produces 40mA current and 5V potential difference. The white light LEDs require  $I_f = 20\text{mA}$  and  $V_f = 4.2\text{V}$ . Obviously, by just connecting a 39  $\Omega$  resistor (for each LED) optimum operating point is reached. The IR light LEDs

require  $I_f = 100\text{mA}$  and  $V_f = 1.5\text{V}$ . Using a  $100\ \Omega$  resistor the optimum voltage is reached, but not the optimum current. There could be used a MOSFET transistor setup to overcome this problem. Although, even if the IR light LEDs “underoperate” when connected as outputs of the microcontroller, their performance is actually adequate for the needs of the system, regarding the close distance between the device and the examinee and the use of 4 IR LEDs (cross topology to have right illumination).

#### *Communication between the components*

The communication between the components is done through signal broadcasting. Typically, everything starts from the user – operator. He triggers the initial signal from the PC, after having initialized the cameras on the bus. This signal activates the camera to start capturing. Then, the camera, through its GPIO pins, triggers the microcontroller to light up the LEDs. Throughout the tests, the IR light LEDs are always on. The white light LEDs are lit for specified time periods, depending on the type of the test. The microcontroller not only sends signals to the LEDs to operate them, but these pulses power them up as well, as said previously. The above is shown on figure 12.

### **3.4 Algorithm and software development**

The software development of the system is concentrated on digital image processing of the pictures acquired. The desired information is the diameter of the pupil. Therefore, an efficient algorithm must be created that will be able to do this operation.

Pupil is normally cycloid. So there is a circle [footprint] that needs to be discovered in each image. In digital image processing theory it is well known that a very efficient algorithm for this problem is the circular Hough Transform;

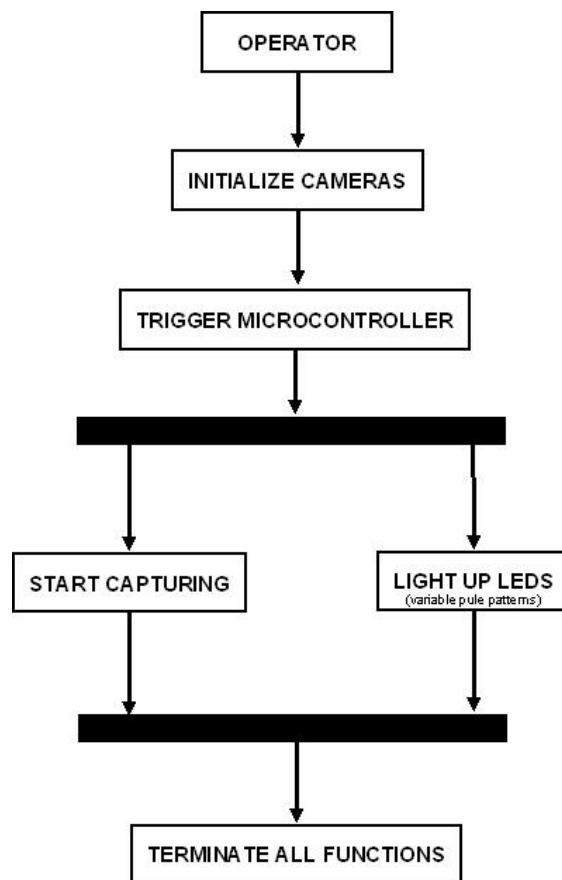


Figure 12 Signal flow diagram

although, it was not the one used in our system due to computational resources and complexity limitations. The explanation has as follows.

A circle is parameterized by its centre coordinates  $(a,b)$  and its radius  $r$ . Then these are related to the position of edge points  $(x,y)$  which form the circle via the equation:

$$(x-a)^2 + (y-b)^2 = r^2$$

This leads to the three dimensional parameter space  $(a,b,r)$ , which belongs to  $\mathbf{R}^3$ . Each point in image space gives rise to a locus of voting points in the 3D Hough space that will be a surface. Therefore, in the 3D Hough space, the locus of

possible parameter values sweeps out the surface of an inverted cone with axis parallel to the  $r$  axis and vertex at  $(a, b, 0)$ .

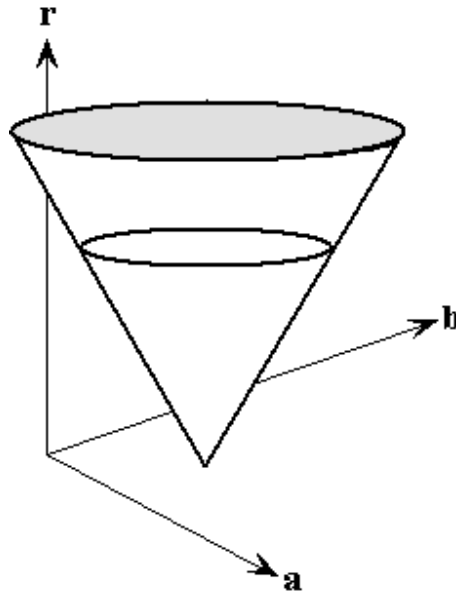


*Figure 13 Parameter space used for circular HT*

The complexity rises as the image size grows. Also CHT by its nature is implemented through nested loops, which are impervious to optimization. The only way to simplify the parametric representation of the circle is to hold the radius as a constant. But this is the information that is searched for in each image (the diameter of the pupil). Practically, the use of CHT in an image demands time and computational resources. In the case of PRIMA system this is unacceptable because of the large size of images, e.g. for a test of 8 seconds duration there are  $8 \times 60 \text{fps} = 480$  images of  $640 \times 480$  size each one. The use of CHT is prohibitive. It was used only as a test tool.

*The above reasons and the relative simplicity of pupil case led to the development of another, very efficient and simple algorithm.*

The images are 8-bit grayscale. This means that each pixel has an intensity value between 0 – 255, where 0 is absolute black and 255 pure white. The pupil, apart from being circular is absolutely black as well (the color in human eyes is

outside from the pupil, in the iris section). So, intuitively, the pupil will be in a very black homogenous area of the image. Based on this fact, the following algorithm was developed, which is inspired by the work of a team from Cuba [15].

*Step 1: Find an initial point inside pupil's area*

To find such a point, someone should not just search a dark pixel area because there may be (and there is quite often) "dark pixel interference" from eyelids and eyebrows. The algorithm initially searches for the maximum sequence of very dark pixels in each row and column of the picture. This process scans dark areas of the image. The threshold below which pixels are categorized as dark is usually under 70. In well focused images and not over-illuminated this might even be at 30. The intersection point of these sequences will be a point in the pupil's area. It won't be a point of something else from the face because only the pupil has an homogenous, or quasi homogenous, surface of black color pixels. Also, this point will not be the center of the circle. Theoretically it should be but in practice it is not, for various reasons, such as the possibility to have white spots from the (infrared in our case) LEDs, or the fact that pupil actually is not a perfect circle.

*Step 2: Find 3 points in pupil's circumference*

Having found a point inside the area of the pupil, an initial point, the next step is to find 3 points in the pupil's contour - or as it is also called the iris inner border. The basic idea for this step is the fact that there is an obvious texture contrast between the pupil and the iris. This implies a statistical difference regarding the values of the pixels of these two areas. Therefore it is appropriated the use of a quantitative texture feature, as the standard deviation, to detect the frontier between the iris and the pupil.

The standard deviation feature is calculated in a point, considering a vicinity of 3x3 pixels size. The standard deviation varies very little inside the pupil area,

however it will suffer an instantaneous abrupt increasing once the vicinity 3x3 begin to take pixels belonging to the iris section. The strategy to find the three points is to extend three trajectories from the initial point to the outer area of the pupil. The trajectories are semi lines, starting from the initial point and directed to the iris. On each point of the trajectory we compute difference between the standard deviation of the initial point and the points of the trajectory. A point whose difference is bigger than a threshold  $P$ , it will be selected as a point of the pupil's contour. The orientations of the trajectories should have a greater or equal than  $90^\circ$  angle, in order to obtain the biggest quantity of information about the contour.

Step 3: *Find the circumference of the pupil.*

Having found 3 points of the pupil's contour on the previous step, from a geometrical point of view, provides an inscribed triangle with known vertices inside the circle that we are looking for. So, geometrically, the problem of finding the radius of the pupil is solved.

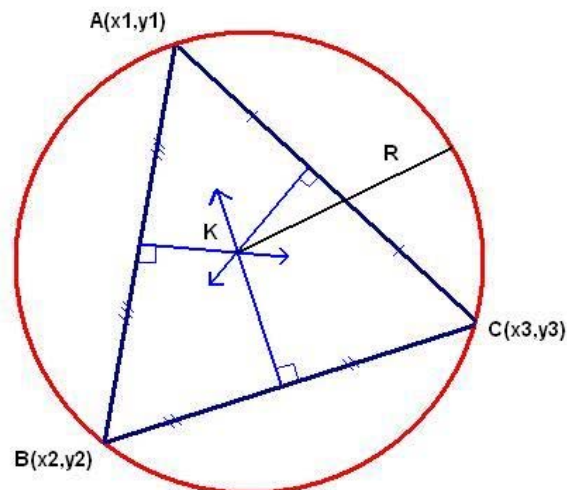
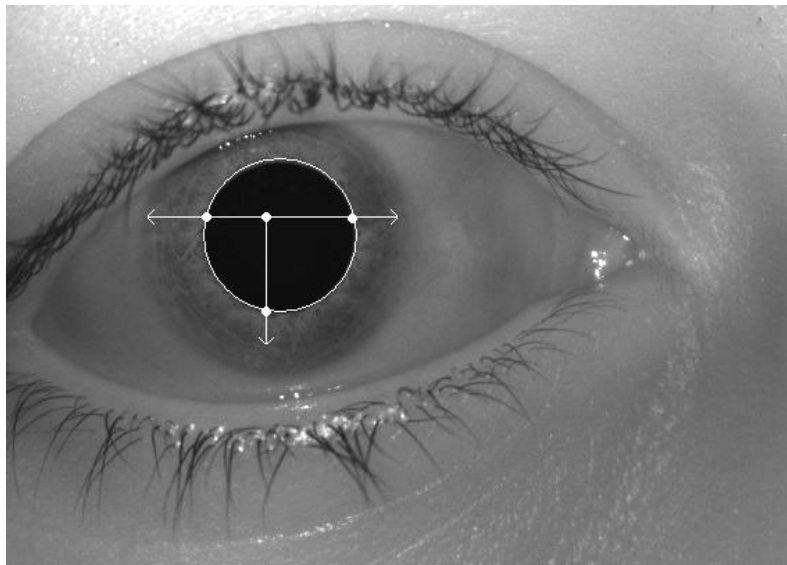


Figure 14 Finding the analytical form of a circle by an inscribed triangle

The points A,B,C are the points found on the 3<sup>rd</sup> step of the algorithm and point K is the center of the circle (pupil). The radius R of the circumscribed circle is calculated from the following formula:

$$R = \frac{\sqrt{(x1-x2)^2 + (y1-y2)^2} \cdot \sqrt{(x3-x1)^2 + (y3-y1)^2} \cdot \sqrt{(x3-x2)^2 + (y3-y2)^2}}{2 \cdot (x2 \cdot y1 - x3 \cdot y1 - x1 \cdot y2 + x3 \cdot y2 + x1 \cdot y3 - x2 \cdot y3)}$$

The center of the circle is the intersection of the 3 mid-vertical sides of the triangle. Its coordinates are found by scanning the pixels of the specific area and search for the one that matches the geometric criteria. The application on a real image is shown below:



*Figure 15 Three point algorithm. Initial point, three points on the contour of the pupil and the resulting circle*

The extended trajectories follow the courses shown above. This approach has the advantage to allow the algorithm to work even when the examinee is about to start to blink or if his eye is semi closed. This procedure is followed for every picture acquired by the system. The software developed is also able to detect

error images by intensity means. For example too dark or too bright images are rejected. From each image the useful information is the diameter of the pupil and this is the only information stored in an array.

In cases of bad focused images or with semi-closed eyes (figure ) the algorithm has potentials of estimating the diameter. For the second case, using CHT would have no results.

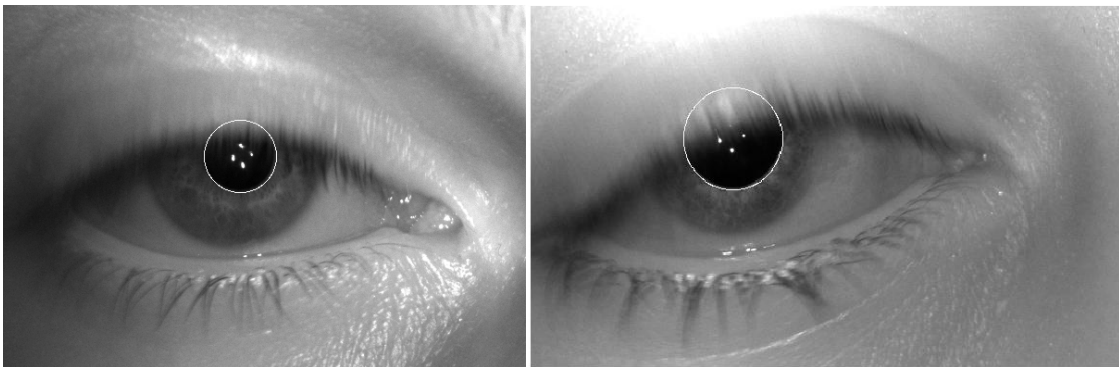


*Figure 16 Semi-closed eyes where the algorithm was successful*

Another scenario where CHT would be unsuccessful is when white spots appeared on pupil's circumference, occurred by the IR LEDs. The edges of the circle in this case are distorted.

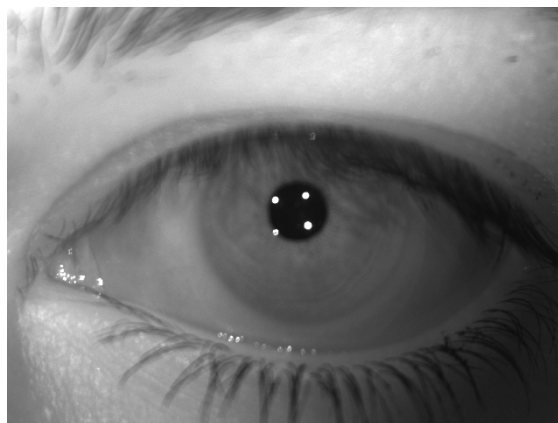


*Figure17 White spot on pupil's contour*

### **3.5 Acquisition method**

The acquisition of the images is done by the camera. The framerate is 60 fps (frames per second), which is the maximum speed of the camera. When acquiring one image, right after the snapshot stage, the data sent to the computer is raw; then it is processed and formatted to the desired filetype. The focusing is done manually. These steps are specified by the operator. The gain of the camera was set to zero, as for not to amplify the noise. The camera provides a high range of flexibility in many ways and stages. The method followed for the acquisition stage is related with the use of custom buffers.

The acquisition of an image demands an earlier memory space allocation. Instead of doing this procedure for each image, which is the default way, another method was used. After initializing the camera on the bus, a number of custom buffers are created and they allocate a block of space needed for the images that are going to be captured. All data is sent and stored in a single file, which grows in size as long as the camera is capturing, through the same custom buffers set at the beginning. This way provides maximum security for the data because the chances of having missed images due to camera register flushes and the time needed for reallocating space are minimized. Also this way uses DMA (direct memory access) for the images through the specified block pointed by the buffers. The resulting file contains the raw data cube of photos and is fragmented to single image files.

When using this method, there are throughput parameters that must be taken into consideration. The maximum amount of padding required is 1 packet, which can be up to 4096 bytes for 1394a and 8192 bytes for 1394b. Adding this padding to the image size will ensure the buffer is large enough to accommodate the image. The needs of the PRIMA system comply with the above limitations.

All the steps from capturing to finally calculating the diameter of the pupil in one image are shown in the following block diagram:

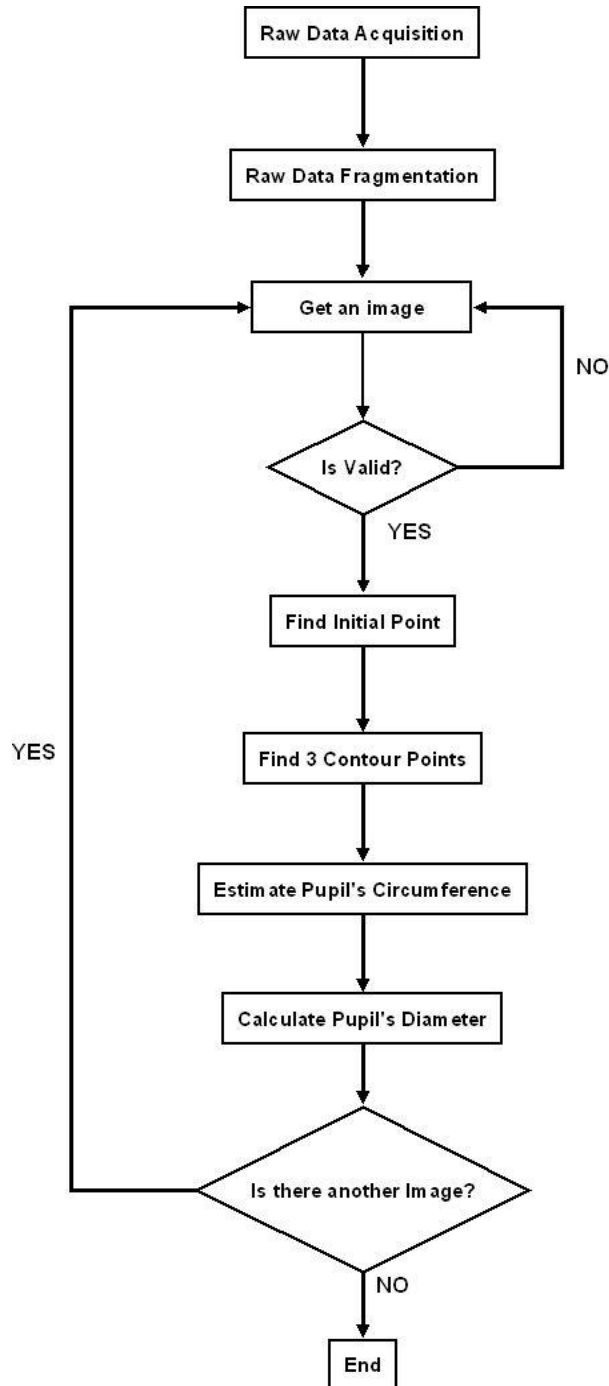
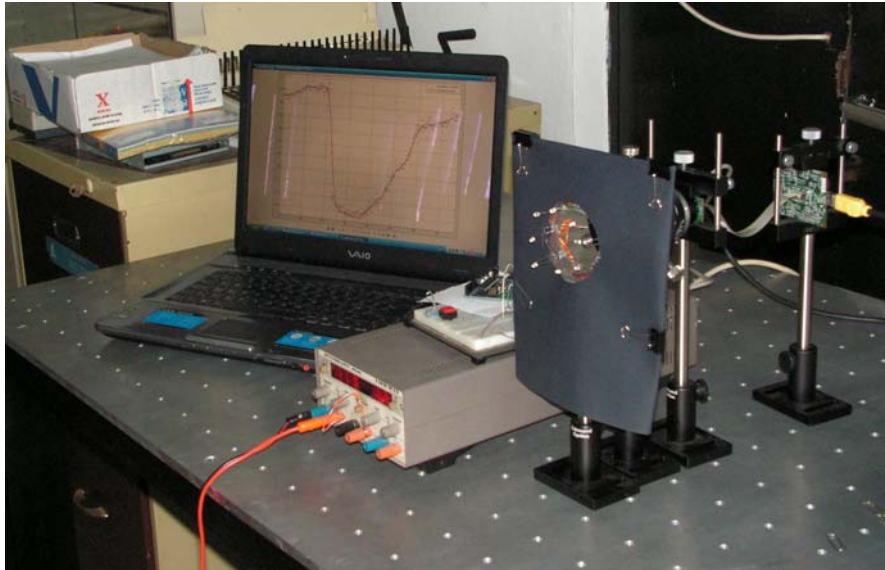


Figure 18 All steps of a PLR test followed by the P.R.I.M.A. system

### 3.6 Experimental Setup

Finally, the experimental setup of the device is as shown below.



*Figure 19 Prototype model developed at the laboratory.*

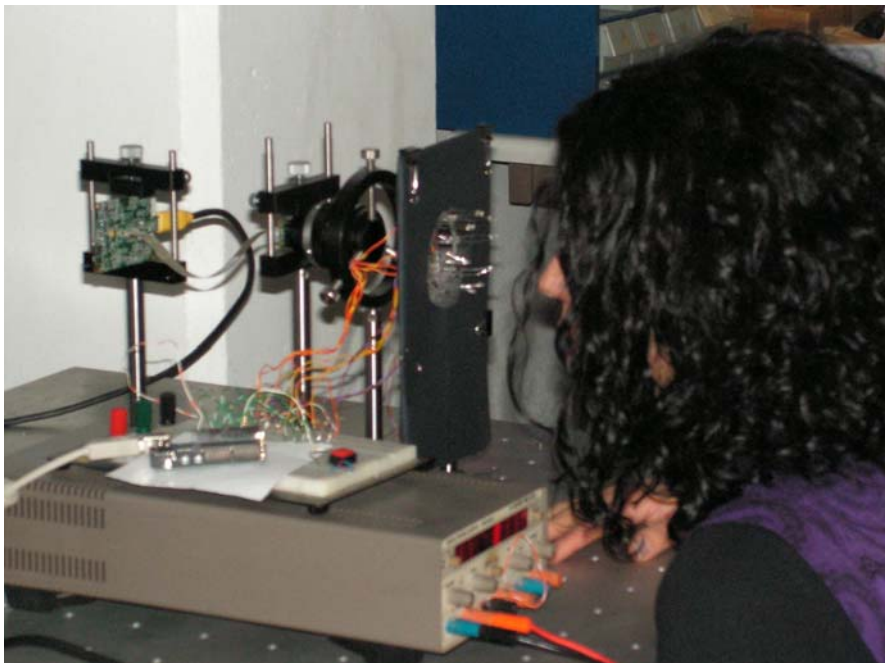


*Figure 20 Demonstration of a test performance. The ambient illumination during a real test must be kept as dark as possible.*

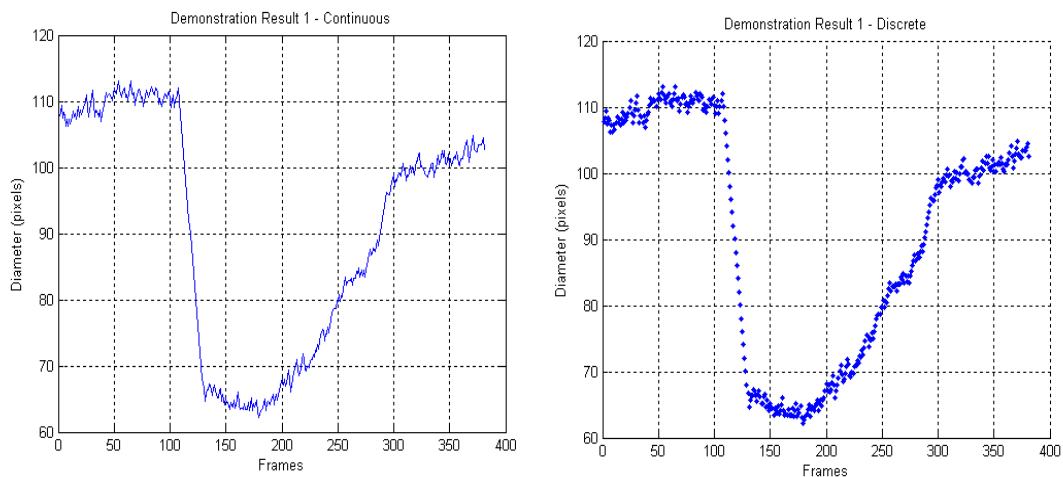
## 4. Results & Conclusions

### 4.1 Subjects and methods

Subjects were staff members who volunteered to test the device. The results shown below are for demonstration purposes only, without any focusing on the medical interpretation of them. They were conducted to test the efficiency of the device.

The position of the examinee is as shown in figures( bla bla) and the ambient illumination should be kept as dark as possible (the ideal is absolute darkness) during the test measurements. This is not only for eliminating the ambient noise, but it is also a requirement of the test as for the maximum pupil dilation.

### 4.2 Pupillograms



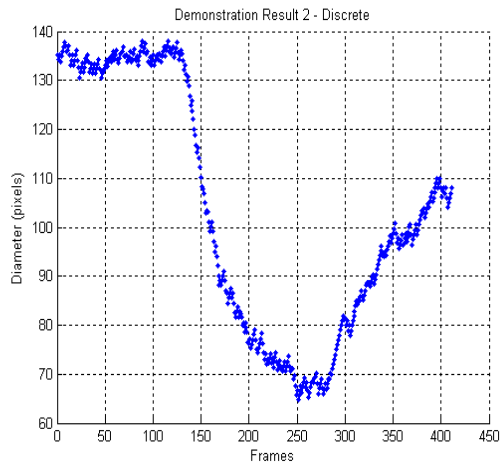
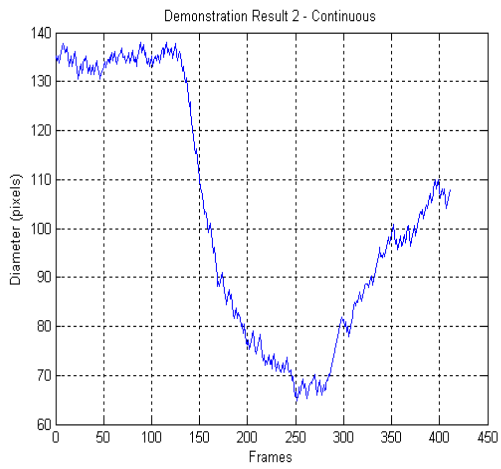


Figure 21 Demonstration Result set1 (morning time)

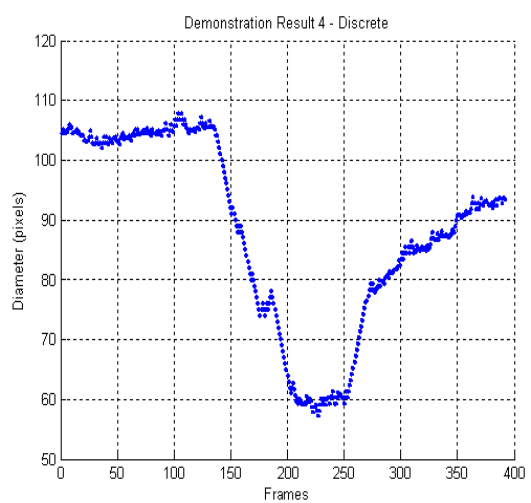
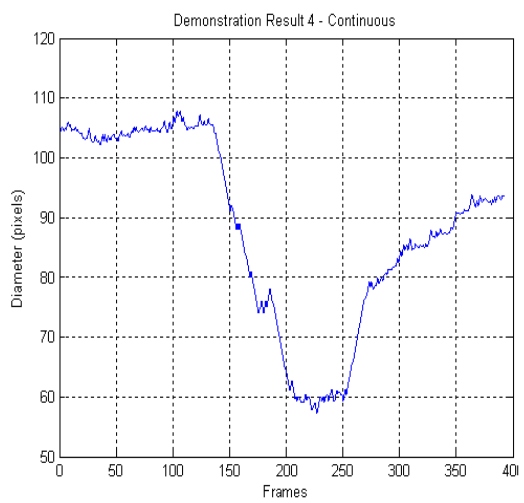
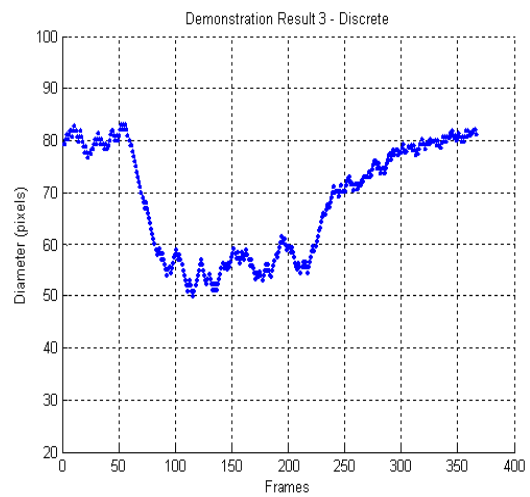
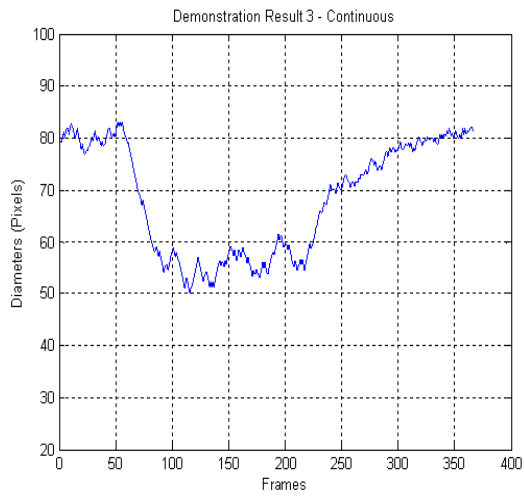


Figure 22 Demonstration Result set2 (late night)

## **Comments on the results**

On the previous diagrams, at the first result set the subjects were tested in the morning. At the second result set the subjects were tested late at night. It is obvious that the pupil adapts with difficulty, as an effect of fatigue.

The fluctuations observed on the results are not only occurred by noise, but other factors are responsible as well. Firstly, the infrared lightning may irritate the pupil and thus, to react with mobility. Secondly, these reactions may be spontaneous. Thirdly, they may be result of a slight anxiety from the examinee. A usual fluctuation is in the range of  $10^{-4}$  m.

Pupillary reflexes are characterized by idiopathy. This means that every person may respond differently to light, in the terms of latency, maximum dilation, minimum constriction etc. It is regarded as impossibility to find people with exactly the same pupillogram.

## **4.3 Mathematical Modeling and Fitting**

In order to elicit valuable information from the acquired data, various calculations need to be done. The resulting dataset, as it is, shows the evolution of the phenomenon in time, maximum dilation and minimum constriction. But there is no direct information about the mobility of the pupil. To calculate these measures, derivation is needed.

As it was mentioned previously, it is impossible to eliminate completely the noise during recording process. Thus the dataset is (slightly) noisy. If the derivative is calculated through finite differences from the discrete dataset, it is going to be very ridging (figure 23). So, to get an analytical expression of the curve and to calculate the slope in every point, curve fitting needs to be done.

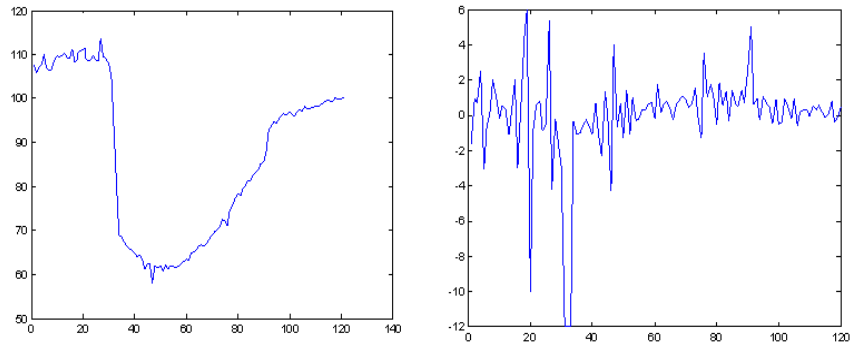


Figure 23 Calculating the first derivative through finite differences

The number of data points, obtained by sampling and experimentation, must be fitted closely by a function. This construction method is called curve fitting or regression analysis or interpolation. The constructed function occasionally goes exactly through the data points, but it also may go between points (poles). The form of the curve, especially when looking at it upside-down, inclines to a combination of Gaussian functions, but this method still maintains rippling, which is unacceptable, and does not always fit well the function (figure 24). The most efficient method to fit and smooth a curve to a set of noisy observations is the “Smoothing Spline”. The splines are a very useful and efficient tool for curve fitting and interpolation.

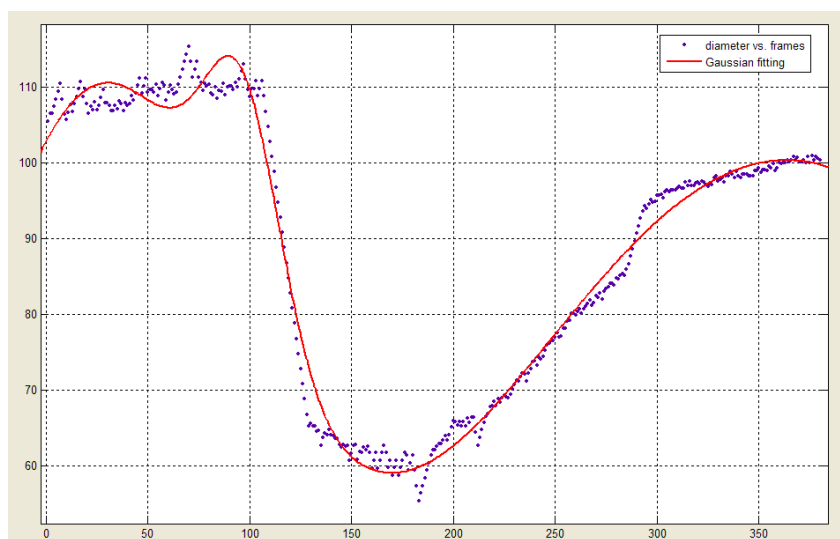


Figure 24 Gaussian fitting on a pupillogram (unsuccessful)

The term "spline" is used to refer to a wide class of functions that are used in applications requiring data interpolation and/or smoothing. The data may be either one-dimensional or multi-dimensional. Spline functions for interpolation are normally determined as the minimizers of suitable measures of roughness (for example integral squared curvature) subject to the interpolation constraints. Smoothing splines may be viewed as generalizations of interpolation splines where the functions are determined to minimize a weighted combination of the average squared approximation error over observed data and the roughness measure. For a number of meaningful definitions of the roughness measure, the spline functions are found to be finite dimensional in nature, which is the primary reason for their utility in computations and representation.

#### 4.3.1 Definition of smoothing splines

Let  $(x_i, Y_i); i = 1, \dots, n$  be a sequence of observations, modeled by the relation  $E(Y_i) = \mu(x_i)$ . The smoothing spline estimate  $\hat{\mu}$  of the function  $\mu$  is defined to be the minimizer (over the class of twice differentiable functions) of

$$\sum_{i=1}^n (Y_i - \hat{\mu}(x_i))^2 + \lambda \int \hat{\mu}''(x)^2 dx.$$

Remarks:

1.  $\lambda \geq 0$  is a smoothing parameter, controlling the trade-off between fidelity to the data and roughness of the function estimate.
2. The integral is evaluated over the range of the  $x_i$ .
3. As  $\lambda \rightarrow 0$  (no smoothing), the smoothing spline converges to the interpolating spline.
4. As  $\lambda \rightarrow \infty$  (infinite smoothing), the roughness penalty becomes paramount and the estimate converges to a linear least-squares estimate.

5. The roughness penalty based on the second derivative is the most common in modern statistics literature, although the method can easily be adapted to penalties based on other derivatives.
6. In early literature, with equally-spaced  $x_i$ , second or third-order differences were used in the penalty, rather than derivatives.
7. When the sum-of-squares term is replaced by a log-likelihood, the resulting estimate is termed *penalized likelihood*. The smoothing spline is the special case of penalized likelihood resulting from a Gaussian likelihood.

### 4.3.2 Derivation of the smoothing spline

It is useful to think of fitting a smoothing spline in two steps:

1. First, derive the values  $\hat{\mu}(x_i); i = 1, \dots, n$ .
2. From these values, derive  $\hat{\mu}(x)$  for all  $x$ .

Treat the second step first.

Given the vector  $\hat{m} = (\hat{\mu}(x_1), \dots, \hat{\mu}(x_n))^T$  of fitted values, the sum-of-squares part of the spline criterion is fixed. It remains only to minimize  $\int \hat{\mu}''(x)^2 dx$  and the minimizer is a natural cubic spline that interpolates the points  $(x_i, \hat{\mu}(x_i))$ . This interpolating spline is a linear operator, and can be written in the form

$$\hat{\mu}(x) = \sum_{i=1}^n \hat{\mu}(x_i) f_i(x)$$

where  $f_i(x)$  are a set of spline basis functions. As a result, the roughness penalty has the form

$$\int \hat{\mu}''(x)^2 dx = \hat{m}^T A \hat{m}.$$

where the elements of  $A$  are  $\int f_i(x) f_j(x) dx$ . The basis functions, and hence the matrix  $A$ , depend on the configuration of the predictor variables  $x_i$ , but not on the responses  $Y_i$  or  $\hat{m}$ .

The penalized sum-of-squares can be written as

$$\|Y - \hat{m}\|^2 + \lambda \hat{m}^T A \hat{m},$$

where  $Y = (Y_1, \dots, Y_n)^T$ . Minimizing over  $\hat{m}$  gives

$$\hat{m} = (I + \lambda A)^{-1} Y.$$

The processing of the data was implemented in Matlab 7.5.0 (R2007b), where the smoothing spline is constructed for the specified parameter  $p$  and the specified weights  $w_i$ . The smoothing spline minimizes

$$p \sum_i w_i (y_i - s(x_i))^2 + (1 - p) \int \left( \frac{d^2 s}{dx^2} \right)^2 dx$$

If the weights are not specified, they are assumed to be 1 for all data points. Parameter  $p$  is defined between 0 and 1.  $p=0$  produces a least squares straight line fit to the data, while  $p=1$  produces a cubic spline interpolant. In this application, the parameter was set to tend to zero to fit the curve more accurately. The choice was subjective, which is an important advantageous ability of using splines because apart from the automatic method, chosen by data, the parameters of smoothing splines may be set manually in order to fit with the expectations of the user as well.

Experimental results of fitting and derivation follow.

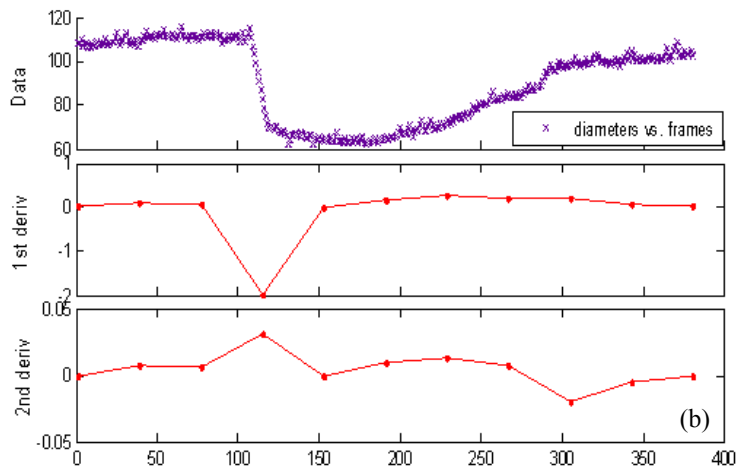
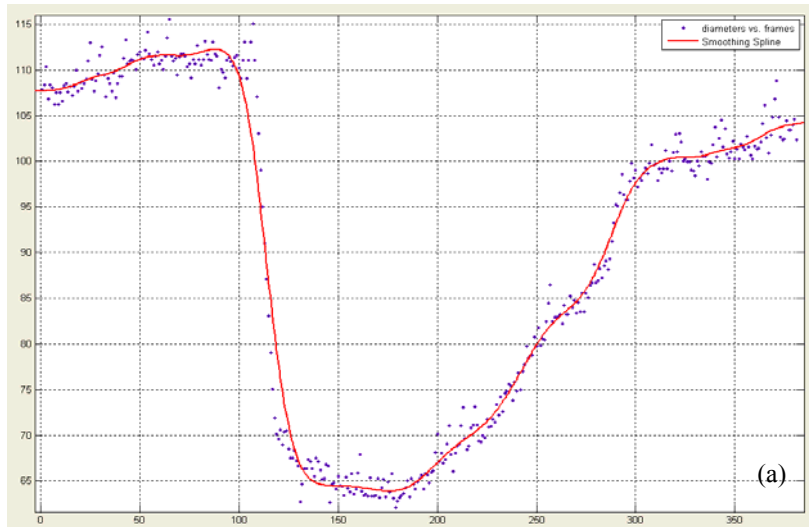


Figure 25 Fitting (a) and derivation (b) using smoothing splines

Frame	Velocity	Acceleration
1	-0.203387	0
39.8	0.0877125	0.0165613
85 <b>max. dilation</b>	0.00687919	0.0184249
117.4	0.431429	0.00858514
156.2	-1.0262	0.0373988
189 <b>max. constriction</b>	-0.629891	0.0240687
233.8	-0.113719	0.00446706
272.6	0.687901	-0.0160429
311.4	0.0229955	-0.0028726
350.2	0.257574	-0.00120264
389	-0.0148594	0

Chart 6 Pupil's velocity and acceleration values on specific frames

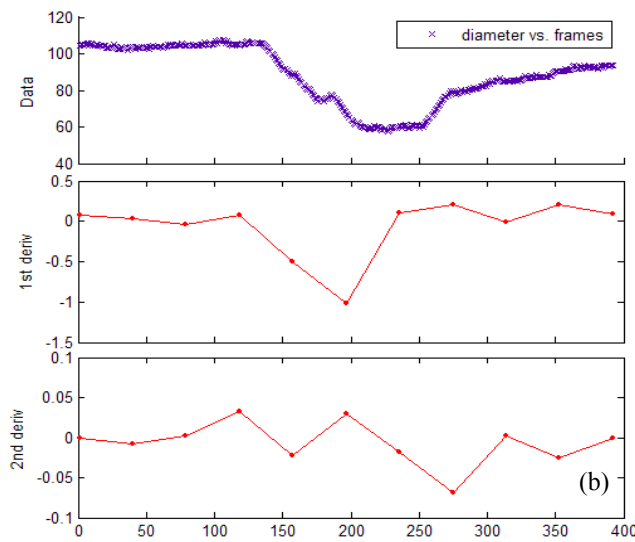
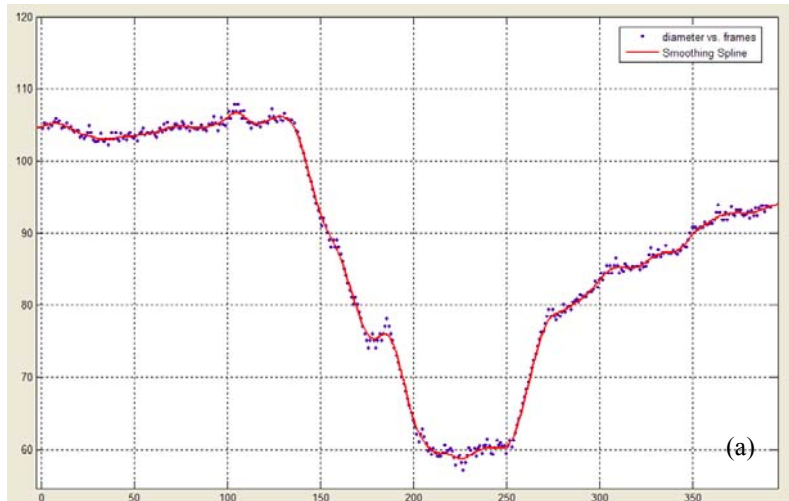
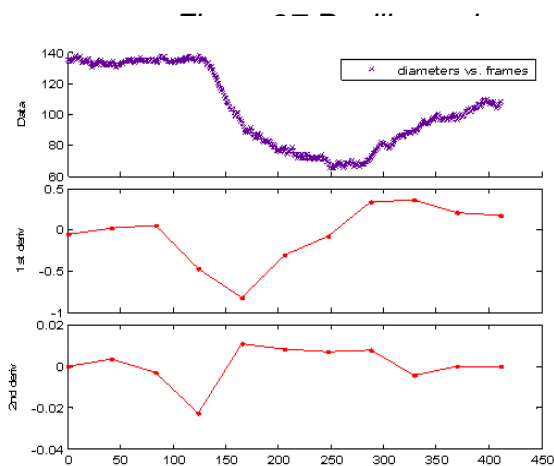
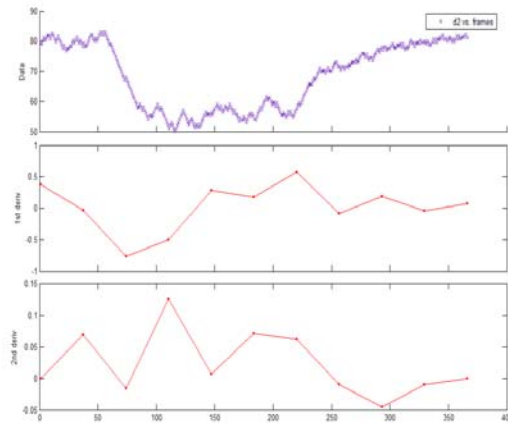
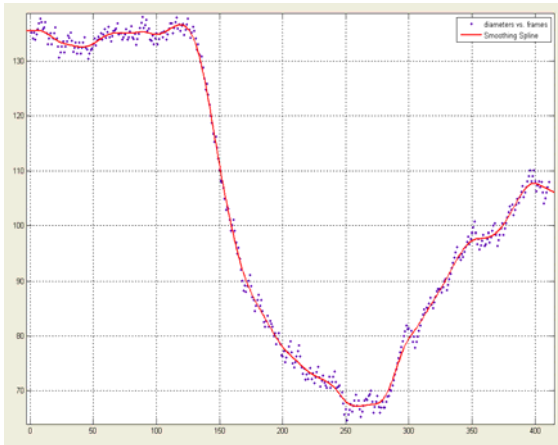


Figure 26 Fitting (a) and derivation (b) using smoothing splines

Frame	Velocity	Acceleration
1	0.0135253	0
39	0.102905	0.00721549
77	0.048419	0.00681621
115 <b>max. dilation</b>	-1.98127	0.0318155
153	-0.00624368	-0.000493668
191	0.173278	0.00940018
229 <b>max. constriction</b>	0.275962	0.0134972
267	0.196078	0.00699904
305	0.203577	-0.0203037
343	0.0558807	-0.00523739
381	0.0347732	0

Chart 7 Pupil's velocity and acceleration values on specific frames



*fitting and derivation examples*

ains a researching field. There is no x phenomenon and thus, no standard neters standardization is yet intuitive. nally discover the “solid” pupillography meter analysis. The following studies demonstrate 3 different ways of interpreting the results of a pupillogram under several circumstances during recent clinical studies. Subjects are not randomly selected, but suffer from a specific disease.

The pupillographic results undoubtedly differ from normal healthy persons. It must be mentioned that these are preliminary reports and the results must be reproduced.

#### 4.4.1 Clinical studies pupillographic results

*F. Fotiou et al./International Journal of Psychophysiology 37 (2000) 111-120*

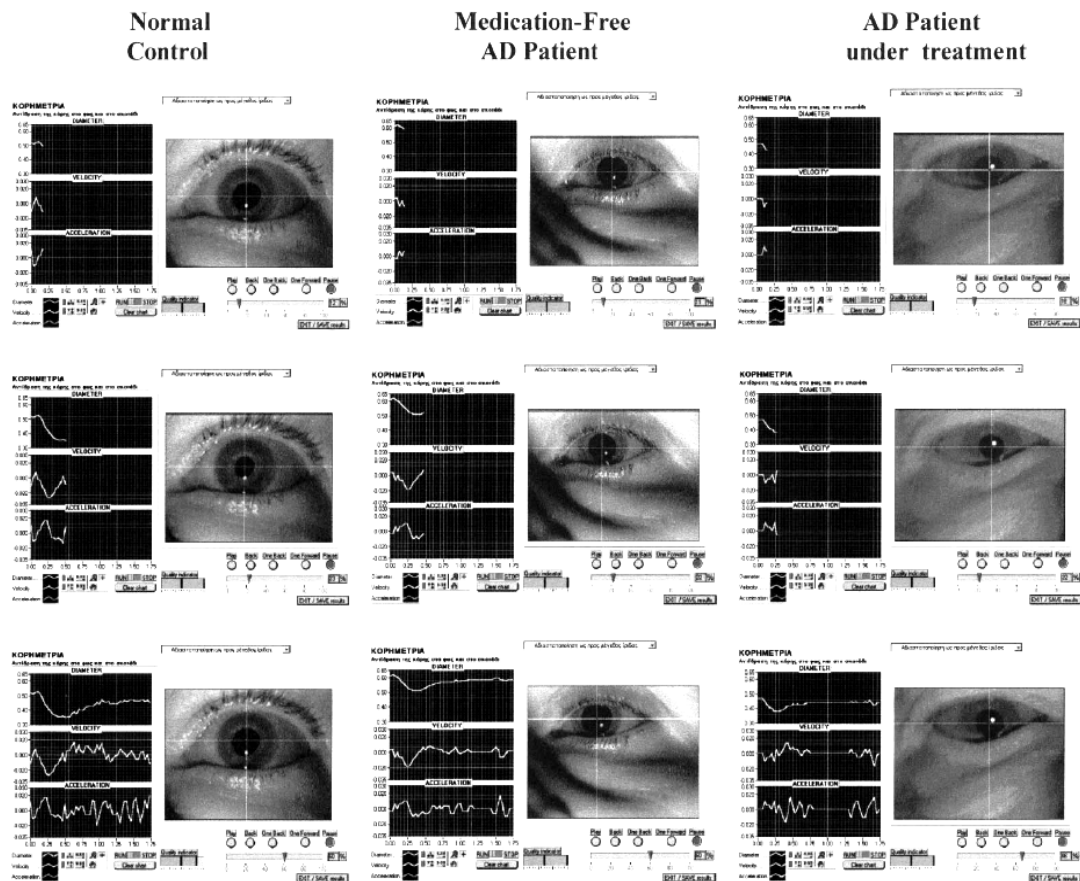


Figure 28 Defect Pupillogram 1.

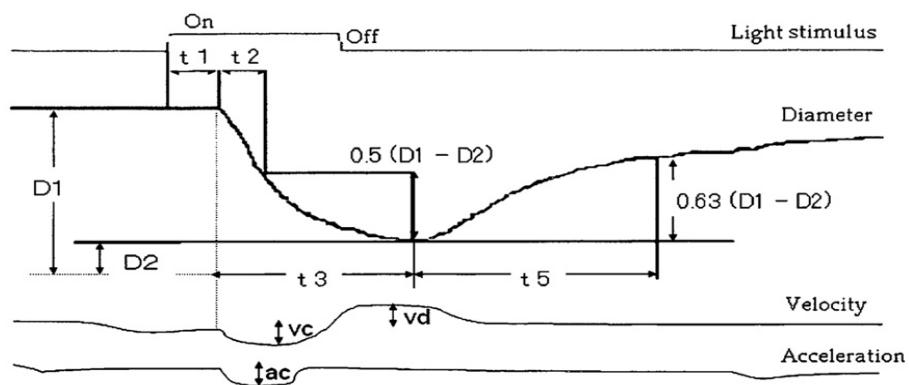
Three different phases of the pupil reaction to light, in a control subject, a medication-free AD patient and an AD patient under medication. Note the

oscillations in the recovery phase of the curve in the normal subject. These oscillations are reduced in both patients.

The results on this study have not been reproduced. Other studies imply different pupillographic factors. Extended research is needed.

**A. Wakasugi et al. / Autonomic Neuroscience: Basic and Clinical 139 (2008)**

**9–14**



- |                        |                                |  |
|------------------------|--------------------------------|--|
| D1: Initial diameter   | t1: Time to constriction       | vc: Maximum velocity of constriction     |
| D2: Minimum diameter   | t2: Time to half constriction  | vd: Maximum velocity of dilatation       |
| CR: Constriction ratio | t3: Time to total constriction | ac: Maximum acceleration of constriction |
| A1: Initial area       | t5: Recovery time              |  |

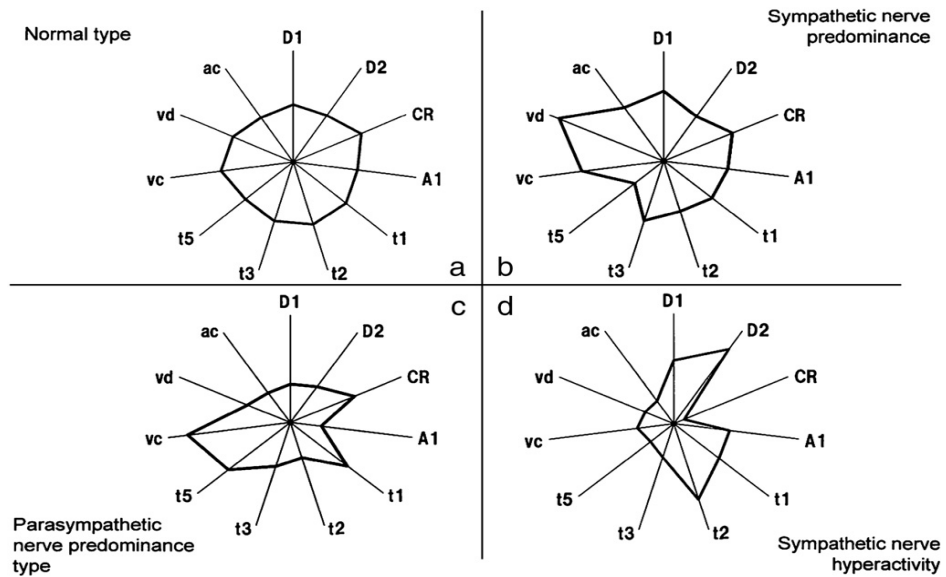


Figure 29 Defect Pupillogram 2. An approach of PLR relative parameters that should be examined during a pupillary response test.

M. Höfle et al. / *International Journal of Psychophysiology* 70 (2008) 171–175

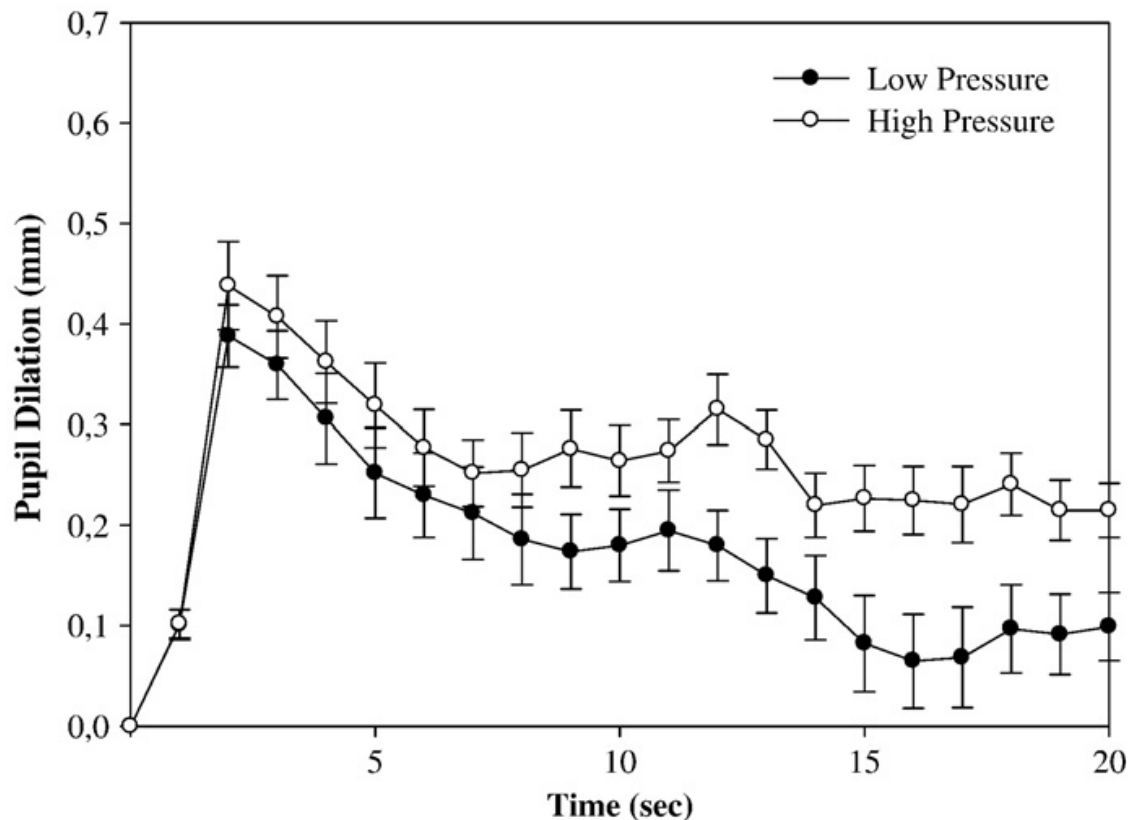


Figure 30 Defect Pupillogram 3. Course of the pupil dilation response from pressure onset until pressure offset differentiated for high and low pressure pain stimuli. Each error bar indicates the range of one standard error

These are some ways of evaluating the results of a pupillary reflexes examination. Under different circumstances, different characteristics of the examinee's ANS and psychological condition may be examined. In this study, pupillary reflexes are observed from a neurological point of view, not

ophthalmological, as to gain a more spherical perspective of the subject. The fact is that pupillary reflexes are not yet standardized and cannot work as a diagnostic mean today, but preliminary reports of pupillography look very promising.

## **4.5 Discussion and conclusions**

Pupil's reaction to light presents a window to the sympathetic and parasympathetic nervous system and is a part of every clinical neurophysiological examination. Despite the popularity, it remains underestimated. It is used mostly to check the reflex's existence (direct and indirect) and the speed, using subjective criteria. The use of infrared capturing in video-pupillometry examination is a relatively low cost, non-invasive, easily performed and sensitive method for testing the ANS functions in humans (and in guinea-pigs). Several studies and clinical surveys have been conducted, either in healthy subjects or patients, since numerous diseases are related with ANS. These were described during the diploma thesis.

Apart from the discussed physiological (e.g. diabetes) and psychophysiological (e.g. depression) diseases related with PLR, other aspects of human health are related also. The sentimentality of a person is expressed (often momentarily) on the pupil. Contentment, pleasure, fear and stressors cause pupillary reflexes. This "psychosensory pupillary response" may be very useful on patients with different psychiatric disorders, who will display different emotional reactions to stimuli presented to them. For example, an alcoholic patient will react differently to the smell of whisky if this patient is a recidivist risk after withdrawal therapy. Also, other psychosomatic aspects of human life may be examined, such as sexuality.

In this study, the pupillary reflexes were evaluated through an extensive bibliographic research on clinical studies. Clinical results presented great interest on the subject and thus, the prototype model was developed in the laboratory. The pupillary reflexes practical tests performance inspired the design. The model

is able of testing various reflexes, as mentioned. It is intended to serve as a novel mean for non-invasive diagnosis and therapeutical methods evaluation. The later is possible because the functionality of ANS, which is previewed through PLR, is responsible for the homeostasis of a person. Homeostasis maintains health stability. Drugs that affect ANS (e.g. antidepressants) are monitored from the PLR point of view. New studies incriminate these drugs that affect the ANS more than the disease itself.

The interpretation of the results is the most important scientific factor that needs to be discussed. Since there is no lateralization on the phenomenon, still numerous surveys need to be conducted in order to reproduce the results. The pupillary reflexes display idiopathy; meaning that every human may respond differently to stimuli in terms of maximum-minimum diameter and adaptation. By processing the results, as seen in Oyamada et al [13], an early objective approach is performed. To elicit information on speed and acceleration, pupil mobility needs to be modeled mathematically. This cannot be accomplished by estimating the finite differences of the dataset, because even small oscillations of the pupil affect the derivation significantly. In this study an approach was made through smoothing splines, a very effective tool on curve fitting. It is ambiguous whether a universal equation will be discovered, able of modeling pupil mobility. Suggestions though, have been provided. Different mathematical approaches are a reason why pupil mobility lacks standardization. Validation of the results in future, is the appropriate method for this purpose.

In conclusion, the significance of pupillary reflexes needs to be emphasized as a neurophysiological, ophthalmological, cognitive, sentimental and awareness meter. Infrared pupillography is an accurate, low-cost, direct and non-invasive method to perform clinical tests. The engineering abilities of the prototype model developed combine numerous functionalities, by allowing a state of customization. It is designed to cover the needs of pupillography in a compact device.

## **4.6 Future Work**

Future work plans of project PRIMA are the compact mounting of the binocular device, with steady and adjustable mechanical parts. The operation of the device, in both hardware and software level, must be promoted to the skills of a non specialized in engineering user, such as a doctor. A critical point is to maintain abilities of flexibility in this initial stage. Close observation on the clinical studies on the subject is crucial. Also, new ways of examining and interpreting the results must be invented, in order to understand the connection between pupillary reflexes and cognitive, awareness and sentimental condition of a human.

## REFERENCES

- [1] H. Wilhelm, B. Wilhelm, "Clinical Applications of Pupillography", *Journal of Neuro-Ophthalmology*, vol. 23, No. 1, 2003.
- [2] Phillips MA, Bitsios P, Szabadi E et al., "Comparison of the antidepressants reboxetine, fluvoxamine and amitriptyline upon spontaneous pupillary fluctuations in healthy human volunteers", *Psychopharmacology (Berlin)* 149(1), pp.72–6, 2000.
- [3] Grünberger J, Linzmayer L, Grunberger M, et al. "Pupillometry in clinical psychophysiological diagnostics: methodology and proposals for application in psychiatry", *Isr J Psychiatry Relat Sci* 1992; 29:100–13.
- [4] F. Fotiou, K.N. Fountoulakis, M. Tsolaki, A. Goulas, A. Palikaras, "Changes in pupil reaction to light in Alzheimer's disease patients: a preliminary report", *International Journal of Psychophysiology* 37, pp 111-120, 2000.
- [5] Greg J. Siegle, Stuart R. Steinhauer, Michael E. Thase, "Pupillary assessment and computational modeling of the Stroop task in depression", *International Journal of Psychophysiology* 52, pp. 63–76, 2004.
- [6] Karl-Jürgen Bär, Michael Karl Boettger, Steffen Schulz, Christina Harzendorf, Marcus Willy Agelink, Vikram K. Yeragani, Prtap Chokka, Andreas Voss, "The interaction between pupil function and cardiovascular regulation in patients with acute schizophrenia", *Clinical Neurophysiology* 119, pp. 2209–2213, 2008.
- [7] J. de Seze, C. Arndt, T. Stojkovic, M. Ayachi, J.Y. Gauvrit, M. Bughin, T. Saint Michel, J.P. Pruvo, J.C. Hache, P. Vermersch, "Pupillary disturbances in multiple sclerosis: correlation with MRI findings", *Journal of the Neurological Sciences* 188, pp. 37–41, 2001.
- [8] A. Keivanidou, D. Fotiou, C. Arnaoutoglou, N. Arnaoutoglou, D. Tsiptsios, D. Partsafyllidis, V. Stergiou, G. Karatasios, A. Karamitrou, A. Karlovasitou, "Changes in pupillary size and mobility in patients with heart failure", *International Journal of Psychophysiology* 69, pp. 242–275, 2008.
- [9] Matthias Du`tsch, Harald Marthol, Georg Michelson, Bernhard Neundorfer, Max Josef Hilz, "Pupillography refines the diagnosis of diabetic autonomic neuropathy", *Journal of the Neurological Sciences* 222, pp. 75–81, 2004.
- [10] Hidetoshi Mori, Shoichi Ueda, Hiroshi Kuge, Eiichi Taniwaki, Tim Hideaki Tanaka, Kiyoshi Adachi, Kazushi Nishijo, "Pupillary response induced by acupuncture stimulation – an experimental study", *Acupuncture in Medicine* 26(2), pp. 79-85, 2008.
- [11] Akino Wakasugi, Hiroshi Odaguchi, Tetsuro Oikawa, Toshihiko Hanawa, "Effects of goshuyuto on lateralization of pupillary dynamics in headache", *Autonomic Neuroscience: Basic and Clinical* 139, pp. 9–14, 2008.
- [12] A. Merzouki, J. Molero Mesa, A. Louktibi, M. Kadiri, G.V. Urbano, "Assessing changes in pupillary size in Rifian smokers of kif (*Cannabis sativa L.*)", *Journal of Forensic and Legal Medicine* 15, pp. 335–338, 2008.

- [13] H. Oyamada, A. Iijima, A. Tanaka, K. Ukai, H. Toda, N. Sugita, M. Yoshizawa, T. Bando, **"A pilot study on pupillary and cardiovascular changes induced by stereoscopic video movies"**, Journal of NeuroEngineering and Rehabilitation, pp. 4:37, 2007.
- [14] H. Wilhelm, **"Neuro-ophthalmology of pupillary function – practical guidelines"**, Journal of Neurology 245, pp. 573–583, 1998.
- [15] J. L. G. Rodríguez, Y. D. Rubio, **"A New Method for Iris Pupil Contour Delimitation and Its Application in Iris Texture Parameter Estimation"**, CIARP 2005, LNCS 3773, pp. 631 – 641, 2005.

## **List of abbreviations**

ANS - Autonomous Nervous System

CHT - Circular Hough Transform

CNS - Central Nervous System

DAN - Diabetes Autonomous Neuropathy

DMA - Direct Memory Access

EEG - Electroencephlography

LED - Light Emitting Diode

PLR - Pupillary Light Reflex

PNS - Parasympathetic Nervous System

PWM - Pulse Width Modulation

SDK - Software Development Kit

SFT - Swinging Flashlight Test

SNS - Symathetic Nervous System

VEP - Visual Evoked Potential

# Appendix

Pupillographic devices. Information obtained by Pupilnet, an internet community of pupil researchers. Other instruments may be available as well.

TABLE 1. *Pupillographic Devices\**

Name of the instrument	CIP	PST	HEY	SWIFT	Visual Pathway Binocular Pupilometer	Micro-measurements System 9000
Manufacturer/distributor	AMTech, <a href="http://www.amtech.de">http://www.amtech.de</a>	AMTech, <a href="http://www.amtech.de">http://www.amtech.de</a>	AMTech, <a href="http://www.amtech.de">http://www.amtech.de</a>	Steinbeis Transferzentrum, Biomed. Optik, <a href="http://www.stz-biomed.de">http://www.stz-biomed.de</a>	Visual Pathways Inc. Prescott, AZ, Ph: +1 928 778 5002	Micro-measurements, Keith Sherman.
Commercially available	Yes	Yes	Yes	Yes	No	No
Principle	IR line scan	IR video	IR video	IR video	IR video and IR reflex	IR video
Spatial resolution	0.01 mm	0.05 mm	na	0.1 mm	0.025	Variable
Temporal resolution	250/125/50/25 Hz	25 Hz	50 Hz	40 ms	60 and 100 Hz	Up to 60 Hz
Online analysis	Yes	Yes	No	Yes	Yes	No
Binocular	No	No	Yes	Yes	Yes	Yes
Light stimulus	Yes	No	Yes	Yes	Yes	Yes
Other stimulus	(Yes)	No	No	No	No	Yes
Application	S, LR, (PS)	SW	S, LR, Com, SW	Com.	S, LR, Com, PP, SW	S, LR, Com, PP, SW
Other features	Horizontal eye movements	Blink count	None	None	Eye movements	Eye movements

*Continued on next page*

TABLE 1. *Continued*

ETS-PC III	Sciscope Pupilometer	The Eyegaze Development System	PUPILSCREEN II® Type 10	PUPILSCAN II® Type 9
ASL Applied Science Laboratory Boston, MA.	Sciscope Instrument Company. Martin Van Orsow, Iowa City, IA. Ph: 319-338-1107 <a href="mailto:martin@sciscope.com">martin@sciscope.com</a>	LC Technologies, <a href="http://www.eyegaze.com">http://www.eyegaze.com</a>	Fairville Medical Optics, Inc., <a href="mailto:brock499@aol.com">brock499@aol.com</a>	Fairville Medical Optics, Inc., <a href="mailto:brock499@aol.com">brock499@aol.com</a>
Yes	Yes	Yes	No (discontinued)	Yes
IR video	IR video	IR video	Scanning OpticRam Image Sensor	Scanning OpticRam Image Sensor
na	Variable	0.5 mm	0.05 mm	0.05 mm
50/60 Hz	na	60 Hz	10 or 20 Hz	10 or 20 Hz
Yes	No	No	Yes	Yes
No	Yes	No	Yes	No
Yes	Yes	No	Yes	Yes
No	Audio	Monitor output	No	No
S, LR, (SW)	S, LR, PS, Com	S, LR, SW	S, LR	S, LR
Eye movements, blink detection	None	Eye movements	None	None

*Continued on next page*

**TABLE 1. Continued**

Name of the instrument	PUPILSCAN II® Model 12	PUPILSCAN II® Model 12A	PUPILSCAN II® Model 129	MonVogl	Octopus 1-2 3 Pupil Perimeter	P_SCAN 100 system
Manufacturer/distributor	Fairville Medical Optics, Inc., brock499@aol.com	Fairville Medical Optics, Inc., lombart@lombartinstrument.com	Fairville Medical Optics, Inc., brock499@aol.com	Metrovision <a href="http://www.metrovision.fr">http://www.metrovision.fr</a>	Interzeag/Clement Clark; Ph: 01 733 6811	City University London, <a href="http://www.city.ac.uk/avrc">http://www.city.ac.uk/avrc</a>
Commercially available	Yes	Yes	No (under development)	Yes	No	Yes (for research projects)
Principle	Scanning CMOS Image Sensor	Scanning CMOS Image Sensor	Scanning CMOS Image Sensor	IR video	IR video	IR video
Spatial resolution	0.05 mm	0.05 mm	0.05 mm	0.05 mm	0.05 mm	0.01 mm
Temporal resolution	10 or 20 Hz	10 Hz	10 or 20 Hz	60 Hz	50 Hz	50–60 Hz
Online analysis	Yes	Yes	Yes	Yes	No	Yes
Binocular	No	No	No	No	No	Yes
Light stimulus	Yes	No	Yes	Yes	Yes	Yes
Other stimulus	No	No	No	Monitor	No	Contrast, color, gratings motion
Application	S, LR	S	S, LR	S, LR, PR, PP, SW	LR, PP	S, LR, PP, SW
Other features	None	None	None	Eye movements	None	Eye movements

*Continued on next page*

**TABLE 1. Continued**

EyeCheck	Chronos Eye Tracker	Procyon P2000SA	Procyon P2000SA	Mayo Clinic Pupillometer	POWERREF II	Oculus Keratograph
MCJ Inc, <a href="http://www.mcjeyecheck.com">http://www.mcjeyecheck.com</a>	Chronos Vision/Skalar Medical <a href="http://www.skalar.nl">http://www.skalar.nl</a>	Procyon Instruments Ltd., <a href="http://www.procyon.co.uk">http://www.procyon.co.uk</a>	Procyon Instruments Ltd., <a href="http://www.procyon.co.uk">http://www.procyon.co.uk</a>	na	Plusoptix AG, <a href="http://www.plusoptix.de">http://www.plusoptix.de</a>	Oculus, <a href="http://www.oculus.de">http://www.oculus.de</a>
Yes	Yes	Yes	Yes	No	Yes	Yes
na	Infrared CMOS imaging	IR video	IR video	IR video	IR video	IR video
na	0.05 mm	0.1 mm	0.1 mm	variable	0.16 mm	0.04 mm
na	50/100/200/400 Hz	5 Hz	25 Hz	60 Hz	12,5/25/50 Hz	8 Hz
na	Yes	Yes	Yes	Yes	Yes	Yes
na	Yes	Yes	Yes	Yes	Yes	No
na	Synchronous output, A/D D/A channel	Yes (3 levels)	Yes (Maxwellian view or closed loop)	Yes	Yes	Yes
na	Synchronous output, A/D D/A channel	No	No	na	No	No
S, LR (used for drug screening)	S, LR, PS, Com, PP, SW	S, LR, Com	S, LR, Com	S, LR, Com, SW	S, LR, Com	S, LR, (Com)
None	Eye movements	na	na	na	Accommodation, Eye movements	Corneal surface analysis

\* Information obtained by E-mail inquiry to Pupil Net: [www.jiscmail.ac.uk/lists/pupil.html](http://www.jiscmail.ac.uk/lists/pupil.html), an internet community of pupil researchers. Other instruments are probably available.

Com, comparison of the two eyes; Hz, Hertz; LR, analysis of light reaction; na, not applicable; PP, pupil perimetry; PS, psychosensory reaction; S, measurement of pupil size; SW, sleepiness waves.